Memoirs of the Faculty of Engineering, Nagoya University
Vol. 30, No. 1. (1978)

ON THE VIBRATIONS OF A SHAFT WITH NONLINEAR SPRING CHARACTERISTICS

TOSHIO YAMAMOTO and YUKIO ISHIDA

Department of Mechanical Engineering

(Received May 30, 1978)

Abstract

When single-row deep groove ball bearings with small angular clearance are used in a rotating shaft system, there appear nonlinear spring characteristics in a restoring force of a shaft. With reference to nonlinear forced oscillations, almost all the researches reported till now is on the topic of rectilinear systems. Nonlinear forced oscillations in a rotating shaft system with gyroscopic moments have unique characteristics. In the first place, we discuss a particular vibration phenomena at the major critical speed when rotating spring characteristics and rotating difference in shaft stiffness exist. In such a case, resonance curves at the major critical speed vary extremely with the change of the angular position of the unbalance and the unstable region appear. Next we consider nonlinear forced oscillations in a shaft system with static nonlinearity. We obtained experimentally various kinds of subharmonic and summed-and-differential harmonic oscillations. It is clarified that the occurrence of these oscillations depends on the assembling condition of the shaft system. Nonlinear forced oscillations are also discussed theoretically. The representation of nonlinear characteristics in polar coordinates gives a clear description of the phenomena and aids in the prediction of the occurrence. It is showed that the experimental results may clearly explained in the light of this theoretical results.

CONTENTS

General Introduction

During the operation of a rotating machine, the shaft sometimes starts to vibrate at special rotating speeds. A large number of research papers have been reported since the paper concerning the dynamics of a rotating shaft was published by Rankine in 1869. Most early literature is concerned with the resonance phenomena which appears when the frequency of external excitation has a specific relationship with the natural frequency of the system. The causes and characteristics of these phenomena have, for the most part, been clarified. Sources of external forces are rotor unbalances, bearing irregularities, etc.

A rotating shaft system with an unsymmetrical rotor or an unsymmetrical shaft has also been studied in detail. In this system, unstable regions appeared at the major critical speeds where the amplitude of whirling oscillation increased exponentially and it became impossible to operate the machine.

Modern rotating machinery is often capable of operating in a high speed region beyond the first critical speed. Consequently, other kinds of phenomena, such as self-excited oscillations and nonlinear oscillations have become serious problems. Self-excited oscillation resultig from internal friction appears in the post-critical range and that due to oil film in journal bearings appears when the rotating speed exceeds twice the major critical speed.

Research on nonlinear oscillations has developed rapidly in the past few decades. As a result, a large number of theoretical and experimental works on nonlinear oscillations have been reported. Almost all of these papers were written about rectilinear systems. Due to the difficulties involved, few papers have been written about the nonlinear oscillations of rotating shafts. There are various reasons for the nonlinearity. The common sources of this nonlinearity are oil film in journal bearings, clearance in ball bearings, magnetic force between the rotor and the stator, and so on. The shapes of resonance curves for these nonlinear phenomena are different from those of linear systems, and oscillations appear which cannot be observed in linear systems. The study of the nonlinear oscillations of rotating shafts started recently and has been slow to develop. One of the authors of this paper, Yamamoto, reported about subharmonic oscillations of order 1/2 and summed-and-differential harmonic oscillations of the type $[p_i \pm p_j]$ (p_i and p_j are the natural frequencies of the system) which were caused by unsymmetrical nonlinear spring characteristics. He observed these whirling oscillations in a rotating shaft system supported by single-row deep groove ball bearings.

In this paper, the various kinds of nonlinear forced oscillations which occurred in a rotating shaft system were studied both experimentally and theoretically. Experiments were conducted using an elastic rotating shaft supported by a single-row deep groove ball bearing and a self-aligning double-row ball bearing. The following is an outline of the chapters.

Chapter 1 describes the particular vibration phenomena which occur at the major critical speed of a shaft system with rotating anisotropies of shaft stiffness and of unsymmetrical nonlinearity. These anisotropies are induced by irregularities in the rotating parts of the shaft system and rotate with the shaft with an angular velocity ω. As a result of these spring characteristics, in the neighborhood of the major critical speed, an unstable region is created or disappears and furthermore resonance curves of the forced oscillations vary grately with the change of the angular position of the unbalance. This paper constitutes the first experimental and theoretical research on the rotating nonlinear spring characteritics of a shaft system.

Chapter 2 clarifies the various nonlinear vibration phenomena which occur in a rotating shaft with static symmetrical nonlinear spring characteristics. A vertical shaft system supported by ball bearings was investigated. When the two center lines of the upper and lower bearings were well aligned and the shaft was situated at the middle of the angular clearance of the single-row deep groove ball bearing, the elastic restoring force of the shaft had symmetrical nonlinear spring characteristics. A subharmonic oscillation of order 1/3 and summed-and-differential harmonic oscillation of the type $[2p_i \pm p_j]$ and $[p_i \pm p_j \pm p_k]$ were obtained with this experimental apparatus. Up till now, no papers have been written about these symmetrical forced oscillations in a rotating shaft system.

In Chapter 3, a theoretical analysis of a rotating shaft system is presented. In a shaft system having a gyroscopic moment, lateral vibrations of the shaft have a mode of whirling motion. In theoretical discussions of this whirling motion, the use

of a polar coordinate system is advocated for the representation of the nonlinear spring characteristics. Nonlinear spring characteristics expressed by polar coordinates can then be classified into a component with a constant value and other components whose magnitudes vary 1, 2, 3, 4, ... times, respectively, while the shaft whirls around its equilibrium position. Equations of the resonance curves are derived theoretically for both subharmonic oscillations and summed-and-differential harmonic oscillations. Utilizing the polar coordinate system, it can be easily be anticipated what kinds of nonlinear forced oscillations can occur. Furthermore, it is demonstrated that the experimental results of Chapter 2 can be clearly explained in the light of the theoretical results obtained in this chapter.

Chapter 1. The Particular Vibration Phenomena Due to Ball Bearings at the Major Critical Speed[1]

1. 1. Introduction

Widely used single-row deep groove ball bearings have so-called "angular clearance[2]". When the center line of the rotating shaft locates within this small angular clearance, the shaft is supported freely. If it goes out from the angular clearance, the supporting condition becomes fixed[2]. (A) When there is a small disalignment between the bearing center line and the center line of the inner cylindrical surface of the bearing box in which the outer ring of the ball bearing is inserted, (B) when the outer ring of the ball bearing is slightly inclined in the bearing box, (C) when there is a raceway run-out of the outer ring raceway, (D) when the inner cylindrical surface of a bearing box is not exactly circular and the fit between the outer ring and the inner surface of the bearing box is loose, etc., the equilibrium position of the center line of the rotating shaft shifts from the center of the angular clearance. As we already reported[2],[3], this shift of the center line of the shaft results in nonuniformity of stiffness and anisotropic unsymmetrical nonlinearity in spring characteristics of the shaft. Consequently, subharmonic oscillations of the order 1/2, summed-and-differential harmonic oscillations, and forced oscillations of synchronous backward precession occur in the shaft system[2]~[6]. As can be seen by (A)~(D), the direction to which the center line of the shaft shifts from the center of the angular clearance is fixed in space. It follows therefrom that the anisotropies of rigidity and of nonlinearity are also fixed in space.

On the other hand, the center line of the shaft also shifts from the center of the angular clearance, (a) when the shaft has a small pre-curvature, (b) when the inner ring of the ball bearing is set to the journal a little inclined, (c) when there is a raceway run-out of the inner ring raceway, (d) when the journal is not exactly circular and the fit between the inner ring and the journal is loose, etc. Accordingly, the anisotropies of shaft stiffness and of unsymmetrical nonlinearity appear in the spring characteristics, and they rotate with the shaft with an angular velocity ω, as seen from (a) ~ (b).

These anisotropies of the spring characteristics rotating with the shaft cause the following phenomena: In the neighborhood of the major critical speed ω_c, an unstable region[7], in which unstable vibrations build up, occurs or disappears as a function of the angular position of the rotor unbalance. The width of this unstable region is also dependent on this angular position. Furthermore, the shapes of the

resonance curves of the forced vibrations caused by the unbalance vary according to the angular position of the unbalance. This chapter clarifies these particular vibration phenomena both analytically and experimentally.

1. 2. Equations of motion

A rather simple rotating shaft system in which a deflection r and an inclination of a rotor do not couple with each other is treated. Initially, the equations of motion of the rotor about its deflection are introduced.

In the preceding section, the anisotropies of stiffness and of nonlinearity rotating with the shaft are discussed. In order to represent such spring characteristics, it is convenient to adopt a rotating rectangular coordinate system $O-x'y'$, which has its origin at the equilibrium position of the center of the rotor and rotates with an angular velocity ω, as shown in Fig. 1. 1. When there is a directional difference in shaft stiffness, the x'-direction of the maximum stiffness is obviously perpendicular to the y'-direction of the minimum stiffness. Unsymmetrical nonlinearity is generally expressed in terms of even powers of the coordinates x' and y', and the second power is considered here. Accordingly, the expression of the potential energy V becomes as follows:

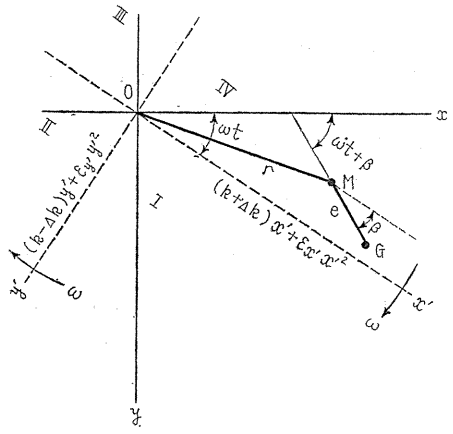

Fig. 1. 1.

$$V=\frac{1}{2}(k+\Delta k)x'^2+\frac{1}{2}(k-\Delta k)y'^2+\beta_1x'^3+\beta_2x'^2y'+\beta_3x'y'^2+\beta_4y'^3 \qquad (1.1)$$

where k is the mean spring constant of the shaft, Δk the difference in shaft stiffness, and $\beta_1\sim\beta_4$ coefficients of nonlinear terms. The spring forces F_x' and F_y' in the x'- and y'-directions are represented by

$$\left.\begin{aligned} F_x'&=-\frac{\partial V}{\partial x'}=-\{(k+\Delta k)x'+3\beta_1x'^2+\underline{2\beta_2x'y'}+\beta_3y'^2\}\\ F_y'&=-\frac{\partial V}{\partial y'}=-\{(k-\Delta k)y'+3\beta_4y'^2+\underline{2\beta_3x'y'}+\beta_2x'^2\}\end{aligned}\right\} \qquad (1.2)$$

respectively, in which the terms underlined are coupling terms between the x'- and y'-directions. We can neglect them and put $\beta_2=\beta_3=0$ in Eq. (1. 2), because the couplings through nonlinear terms are considered small and experimental results discussed later can be explained almost completely without them. By putting $3\beta_1=\varepsilon_x'$, $3\beta_4=\varepsilon_y'$ Eq. (1. 2) becomes

$$F_x'=-\{(k+\Delta k)x'+\varepsilon_x'x'^2\},\quad F_y'=-\{(k-\Delta k)y'+\varepsilon_y'y'^2\} \qquad (1.3)$$

In Fig. 1. 1, $O-xy$ is a fixed rectangular coordinate system, M(x', y') is the

geometrical center of the rotor, $G(x'_G, y'_G)$ is the center of gravity of the rotor, $MG=e$ is the eccentricity of the rotor, and the next relations hold,

$$x'_G=x'+e\cdot\cos\beta,\quad y'_G=y'+e\cdot\sin\beta \tag{1.4}$$

where β is the angle between the direction of the eccentricity and the x'-direction. When viscous damping forces $D_x=-c\dot{x}$, $D_y=-c\dot{y}$ (c: damping coefficient), which are expressed in the fixed coordinate system, act upon the system, the damping forces D_x' and D_y' in the x'- and y'-directions are expressed as follows:

$$D'_x=-c\dot{x}'+c\omega y',\quad D'_y=-c\dot{y}'-c\omega x' \tag{1.5}$$

Let the mass of the rotor be m. Then the inertia forces in the x'- and y'-directions are given by $(-m\ddot{x}'_G+2m\omega\dot{y}'_G+mx'_G\omega^2)$ and $(-m\ddot{y}'_G-2m\omega\dot{x}'_G+my'_G\omega^2)$ respectively in the rotating coordinate system. By using D'Alembelt's principle, the following equations of motion are introduced:

$$\left.\begin{aligned}&(-m\ddot{x}'_G+2m\omega\dot{y}'_G+mx'_G\omega^2)+(-c\dot{x}'+c\omega y')-\{(k+\Delta k)x'+\varepsilon'_x x'^2\}=0\\&(-m\ddot{y}'_G-2m\omega\dot{x}'_G+my'_G\omega^2)+(-c\dot{y}'-c\omega x')-\{(k-\Delta k)y'+\varepsilon'_y y'^2\}=0\end{aligned}\right\} \tag{1.6}$$

where Δk, ε'_x, ε'_y, and c are small quantities. We express the forced vibrations caused by the eccentricity e, that is, the harmonic solutions of frequency ω, as

$$\left.\begin{aligned}x&=A\cos(\omega t+\alpha)=b\cos\omega t-a\sin\omega t\\y&=A\sin(\omega t+\alpha)=b\sin\omega t+a\cos\omega t\end{aligned}\right\} \tag{1.7}$$

where

$$a=A\sin\alpha,\quad b=A\cos\alpha \tag{1.8}$$

are functions of time t. Since Δk, c, ε'_x, and ε'_y are small, $\dot{a}$ and $\dot{b}$, $\ddot{a}$ and $\ddot{b}$ are small quantities of the first and the second order respectively. By comparing the relations $x=x'\cos\omega t-y'\sin\omega t$, $y=x'\sin\omega t+y'\cos\omega t$ with Eq. (1. 7), we get

$$x'=b,\quad y'=a \tag{1.9}$$

Substituting Eqs. (1. 4) and (1. 9) into Eq. (1. 6), and neglecting the second or higher orders of small quantities, we obtain

$$\left.\begin{aligned}2m\omega\dot{a}&=-\{m\omega^2-(k+\Delta k)\}b+\varepsilon'_x b^2-c\omega a-me\omega^2\cos\beta\\2m\omega\dot{b}&=\{m\omega^2-(k-\Delta k)\}a-\varepsilon'_y a^2-c\omega b+me\omega^2\sin\beta\end{aligned}\right\} \tag{1.10}$$

1. 3. Harmonic oscillations and stability criteria

Denoting the steady state solutions of harmonic oscillations by a_0 and b_0, and putting $\dot{a}=0$, $\dot{b}=0$, $a=a_0$, and $b=b_0$ in Eq. (1. 10), we obtain the following equations:

$$\left.\begin{aligned}&\varepsilon'_x b_0^2-m\sigma_1 b_0-me\omega^2\cos\beta=c\omega a_0\\&-\varepsilon'_y a_0^2+m\sigma_2 a_0+me\omega^2\sin\beta=c\omega b_0\end{aligned}\right\} \tag{1.11}$$

where

$$\sigma_1=\omega^2-p^2(1+\Delta k/k),\quad \sigma_2=\omega^2-p^2(1-\Delta k/k) \tag{1.12}$$

are detunings, and $p=\sqrt{k/m}$ is the natural frequency of the system. From Eq. (1. 11), a_0, b_0, hence the stationary amplitude of harmonic oscillation $A_0=\sqrt{a_0{}^2+b_0{}^2}$ can be determined.

In order to investigate stability problems of forced vibrations, we transform Eq. (1. 10) into

$$\frac{db}{da}=\frac{m\sigma_2 a-\varepsilon'_y a^2-c\omega b+me\omega^2\sin\beta}{-m\sigma_1 b+\varepsilon'_x b^2-c\omega a-me\omega^2\cos\beta} \tag{1.13}$$

If we substitute

$$a=a_0+\xi,\quad b=b_0+\eta \tag{1.14}$$

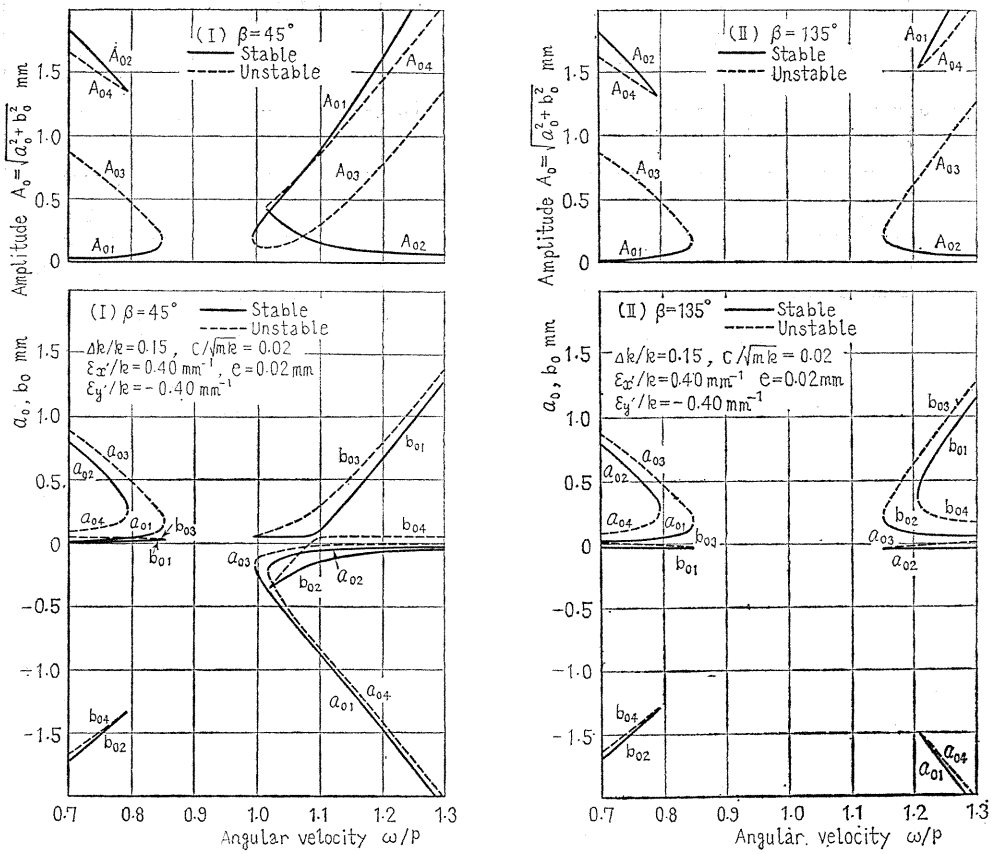

Fig. 1. 2. Resonance curve (eccentricity e is located in quadrant I, US-type)

Fig. 1. 3. Resonance curve (eccentricity e is located in quadrant II, UU-type)

Δk : directional difference in shaft stiffness, k : mean spring constant,
ε'_x, ε'_y : coefficients of nonlinear terms, m : mass of the rotor,
c : damping coefficient, e : eccentricity

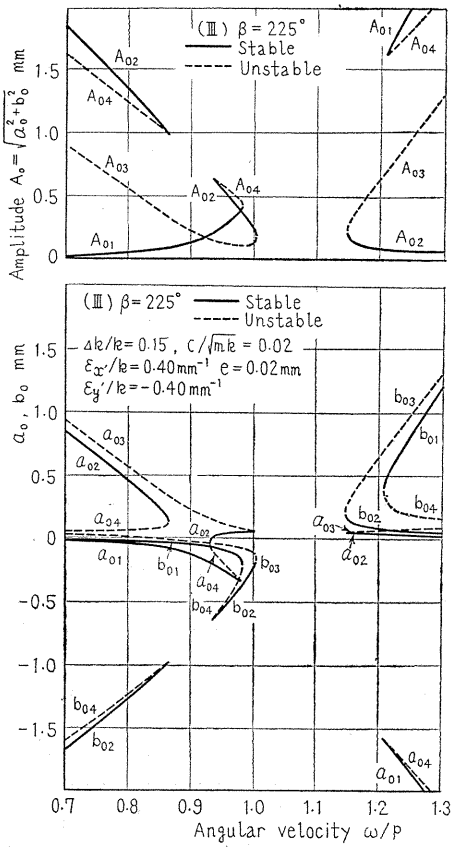

Fig. 1. 4. Resonance curve (eccentricity e is located in quadrant Ⅲ, SU-type)

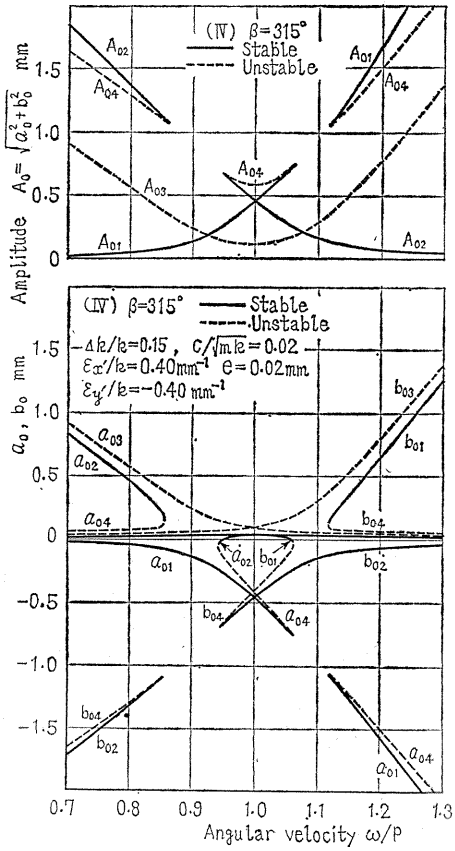

Fig. 1. 5. Resonance curve (eccentricity e is located in quadrant Ⅳ, SS-type)

into Eq. (1. 13) and reject all but linear terms for the small deviations ξ and η, we obtain

$$\frac{d\eta}{d\xi}=\frac{(m\sigma_2-2\varepsilon'_y a_0)\xi-c\omega\eta}{-c\omega\xi-(m\sigma_1-2\varepsilon'_x b_0)\eta}=\frac{a^*\xi+b^*\eta}{c^*\xi+d^*\eta} \tag{1.15}$$

In the stability conditions $b^*+c^*=-2c\omega<0$ and $a^*d^*-b^*c^*<0$, the former always holds, so the following equation obtained from the latter represents the stability condition:

$$(m\sigma_1-2\varepsilon'_x b_0)(m\sigma_2-2\varepsilon'_y a_0)+c^2\omega^2>0 \tag{1.16}$$

In Figs. 1. 2~1. 5, we show resonance curves in the neighborhood of the resonance point $p=\omega$, which are calculated by Eq. (1. 11) for the four cases $\beta=45°$, 135°, 225°, and 315°. They are the cases in which the eccentricity e is located in the middle of each of the four quadrants divided by the x'-and y'-axes, as shown in Fig. 1. 1. In general, a_0 and b_0 have four values for a given angular velocity ω of the shaft, and we distinguish these by the symbols a_{0i}, b_{0i}, and $A_{0i}=\sqrt{a_{0i}^2+b_{0i}^2}$

($i=1\sim4$). Resonance curves for $\Delta k/k=0.15$, $\varepsilon'_x/k=0.40\text{mm}^{-1}$, $\varepsilon'_y/k=-0.40\text{mm}^{-1}$, $c/\sqrt{mk}=0.02$, and $e=0.02$mm are illustrated in Figs. 1. 2~1. 5. Signs of the coefficients ε'_x, ε'_y of nonlinear terms have no substantial effect on vibration characteristics. In Figs. 1. 2~1. 5, resonance curves for the case of $\varepsilon'_x>0$ and $\varepsilon'_y<0$ are shown, because the experiments explained later are performed when $\varepsilon'_x>0$ and $\varepsilon'_y<0$. Signs of ε'_x and ε'_y are determined easily from measurements of spring characteristics (e. g. Fig. 1. 13). In Figs. 1. 2~1. 5, solid line and broken line curves mean stable and unstable vibrations, respectively.

In Figs. 1. 2~1. 5, the ranges of the angular velocity ω for which no solid line curve A_{0i} exists indicate unstable regions, where unstable vibrations of frequency ω occur and their amplitudes increase exponentially. Unstable regions take place in Figs. 1. 2, 1. 3, and 1. 4, which show the resonance curves for the cases when the eccentricity is located in the quadrants Ⅰ, Ⅱ, and Ⅲ, respectively. The unstable region disappears when the eccentricity is located in quadrant Ⅳ, as shown in Fig. 1. 5. In Fig. 1. 3, where e is located in quadrant Ⅱ, the widest unstable region appears. In Fig. 1. 2 (e is located in quadrant Ⅰ) and in Fig. 1. 4 (e is located in quadrant Ⅲ), the unstable region becomes narrower from the higher speed side and the lower speed side, respectively. Solid line curves A_{01} and A_{02} cross each other in Fig. 1. 5. At the point of intersection, both curves have equal amplitudes but unequal phases.

From Fig. 1. 6, we can understand why the angular position β of the eccentricity has influence on vibrations, i. e., on the shapes of the resonance curves, on the width of the unstable region and on its location, etc., as shown in Figs. 1. 2~1. 5. Since only the A_{01}-curve of the lower speed side and the A_{02}-curve of the higher speed side are obtained experimentally, as we will show later, we are going to investigate them. For brevity, we consider the case that $c=0$. From Eq. (1. 11), we can see the following: When e is located in quadrants Ⅰ and Ⅱ, $\sin\beta$ is positive, and hence a_0 (>0) of the lower speed side lies along the holizontal line $a_0=0$, turns at point A, and approaches the straight line $m\sigma_2-\varepsilon'_y a_0=0$ asymptotically, like the a'_{01}-curve shown in the figure. When e is located in quadrants Ⅲ and Ⅳ, $\sin\beta$ is negative, and hence a_0 (<0) approaches the straight line $m\sigma_2-\varepsilon'_y a_0=0$ asymptotically, like the a_{01}-curve. The b_0-curve of the higher speed side becomes the b_{02}- or b'_{02}-curve which approaches the straight line $m\sigma_1-\varepsilon'_x b_0=0$ asymptotically, according to the sign of $\cos\beta$, that is, according to whether e is located in quadrants Ⅰ, Ⅳ or in quadrants Ⅱ, Ⅲ. The curves which turn are indicated by the symbol U, and those which do not are indicated by the symbol S. By considering values of magnification factors, it can be seen that the amplitude $A_0=\sqrt{a_0^2+b_0^2}$ is almost equal to a_0 on the lower speed side, and to b_0 on the higher speed side. Accordingly when e is located in quadrant Ⅰ, the A_0-curve becomes almost like a'_{01} (U) on the lower speed side and like b_{02} (S) on the higher speed side, hence a resonance curve of the US-type shown in Fig. 1. 2 is formed. When e is located in quadrant Ⅱ, the A_0-curve becomes like a'_{01} (U) and b'_{02} (U), thus a

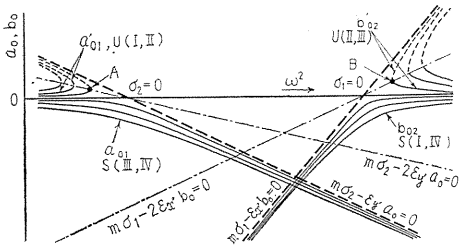

Fig. 1. 6. ($\varepsilon'_x>0$, $\varepsilon'_y<0$, Ⅰ-US, Ⅱ-UU, Ⅲ-SU, Ⅳ-SS)

resonance curve of the UU-type shown in Fig. 1. 3 appears. In the similar way, it can be concluded that, when e is located in quadrants Ⅲ and Ⅳ, resonance curves of the SU- and SS-types shown in Fig. 1. 4 and Fig. 1. 5 appear. It can be seen obviously that the UU-type has the widest unstable region, and in cases of the SU- and US-types, unstable regions become narrower from the lower speed side and the higher speed side, respectively.

Depending on the signs of the coefficients ε_x', ε_y' of the nonlinear terms, the relation beween the quadrant in which the eccentricity is located and the type of resonance curve changes as shown in Table 1. 1.

Table 1. 1.

ε_x'	ε_y'	the quadrant in which eccentricity is located			
		Ⅰ	Ⅱ	Ⅲ	Ⅳ
+	+	SS	SU	UU	US
+	−	US	UU	SU	SS
−	+	SU	SS	US	UU
−	−	UU	US	SS	SU

In the assembling of the experimental apparatus, certain conditions can be achieved so that the spring characteristics of $\varepsilon_x'\simeq 0$, $\varepsilon_y'>0$ result. When $\varepsilon_x'\simeq 0$, $\varepsilon_y'>0$, properties of vibrations change according to whether e is located in Ⅰ, Ⅱ ($\beta\simeq 0°\sim 180°$) or in Ⅲ, Ⅳ ($\beta\simeq 180°\sim 360°$). In the former case, the resonance curves become as shown in Fig. 1. 7 ($\beta=90°$), and in the latter, they are as in Fig. 1. 8 ($\beta=270°$), where there is a wide unstable region. Resonance curves obtained analytically for $\Delta k/k=0.15$, $\varepsilon_x'/k=0$, $\varepsilon_y'/k=0.56\text{mm}^{-1}$, $c/\sqrt{mk}=0.02$, and $e=0.02$ are shown in Figs. 1. 7 and 1. 8. Figure 1. 9 shows in more detail the relation between the angular position β of eccentricity and the unstable region. For example, where, β is 225°, the regions between a and b, c and d are unstable ones. We can see from the figure that a wide unstable region appears when $\beta\simeq 180°\sim 360°$. Incidentally, a narrow unstable region also exists in the range of $\omega/p\simeq 1.06\sim 1.08$.

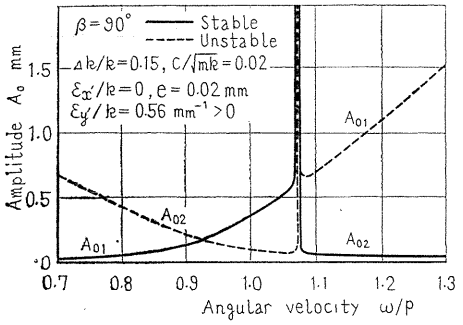

Fig. 1. 7. Resonance curve (nonlinearity exists only in the y'-direction)

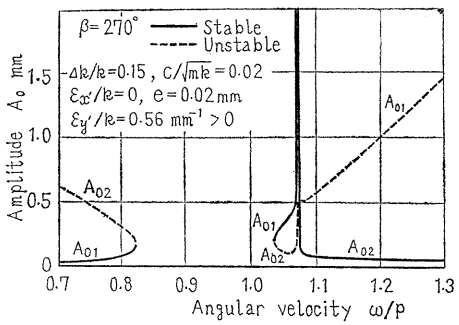

Fig. 1. 8. Resonance curve (nonlinearity exists only in the y'-direction)

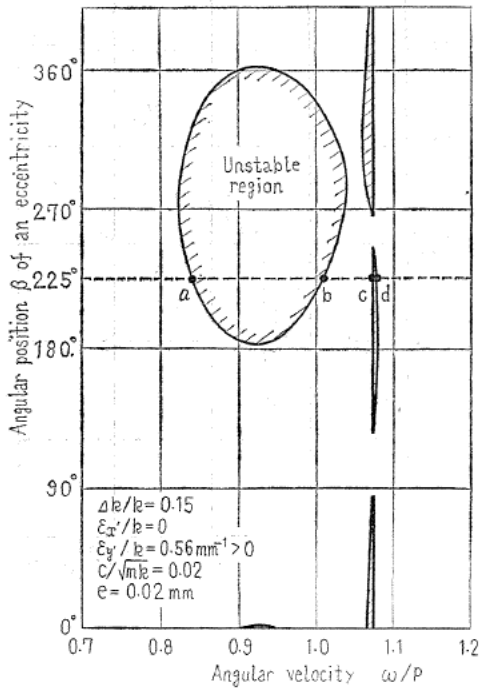

Fig. 1. 9. Relation between the angular position β of eccentricity and the unstable region

1. 4. Experimental apparatus and experimental results

As shown in Fig. 1. 10, a circular disc R is mounted on a rotating shaft S with a circular cross section at the position $a : b = 1 : 4$ (a=140mm, b=560mm). The diameter of the shaft is 11. 98mm, and its length l is 700mm. Dimensions of the disc are 481. 3mm in diameter, 5. 55mm in thickness, and 7. 87kg in weight. The shaft is supported by a self-aligning double-row ball bearing (#1200) at the upper end, and by a single-row deep groove ball bearing (#6204) at the lower end. Lateral deflections of the disc edge in the x- and y-directions are recorded by an optical system, and rotation marks are made by a small paper P. Since the distance a is not equal to b and the deflections and the inclinations of the rotor couple with each other in the rotating shaft system of Fig. 1. 10, it is not such a simple system as the one treated in the preceding section. However, so far as the problem is confined to forced vibrations of frequency ω, that is, harmonic solutions in the neighborhood of the major critical speed, the conclutions of the preceding section can be applied to the system shown in Fig. 1. 10 without any modification.

If there exists an anisotropy of shaft stiffness Δk, the shaft can be considered a flat one. Consequently, when the nonrotating shaft is hit, two free vibrations with the frequencies p_{01} and p_{02}, which correspond to the shaft stiffnesses $k+\Delta k$ and $k-\Delta k$ respectively, occur simultaneously, and a beat phenomenon appears. When it is hit in the x'-direction or the y'-direction, however, only one free vibration with the frequency p_{01} or p_{02} takes place. Performing experiments in such a way, we can determine the angular positions of the x'- and y'-directions and the values of p_{01} and p_{02}. Experiments are performed for various angular positions Θ (Fig. 1.10) of the rotor. The experimental results are illustrated in Figs. 1.11 and 1.12. In Fig.

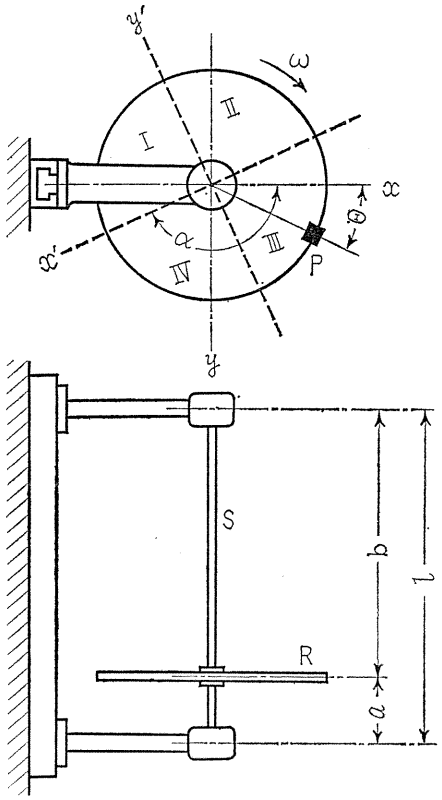

Fig. 1. 10. Experimental apparatus

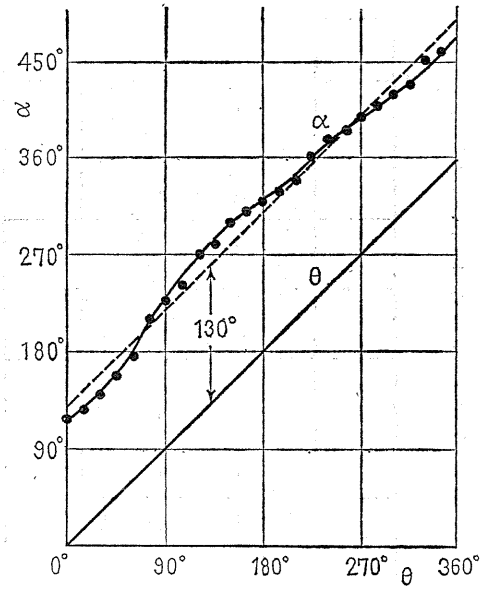

Fig. 1. 11. Relation between the angular position α of the x'-direction and the angular position θ

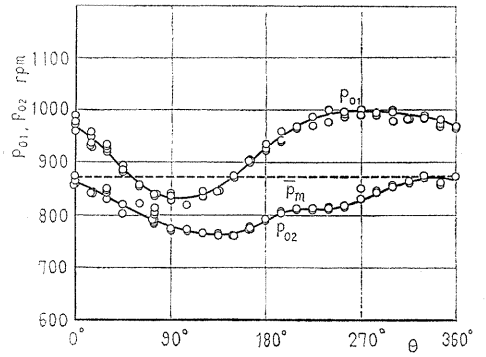

Fig. 1. 12.

1. 11, we show the relation between the angular position α of the x'-direction and the angular position θ, where the x'-direction always goes ahead of the small paper P by about 130°. It follows that the x' -direction, i. e. the direction of shaft stiffness $(k+\Delta k)$, and the y'-direction, i. e. that of $(k-\Delta k)$, rotate with the shaft like a flat shaft, and the x'-direction is perpendicular to the y'-direction. In Fig. 1. 12, values of the natural frequencies p_{01} and p_{02} in the x'- and y'-directions, respectively, are plottd against the angular position of the disc θ. The frequencies p_{01}, p_{02}, the mean value $p_m=(p_{01}+p_{02})/2$, and the difference $p_d=(p_{01}-p_{02})/2$ change with θ. Accordingly, we can see that not only the rotating anisotropy, but also the anisotropy fixed in space, caused by (A)～(D) in Section 1. 1, exists. From Fig. 1. 12, the average values of p_m and p_d, $\bar{p}_m$ and $\bar{p}_d$, can be obtained, and we have $\bar{p}_m\simeq 872$ rpm and $\bar{p}_d\simeq 57.5$ rpm.

In the analysis in the preceding section, we assumed that the spring constant k and the directional difference of the spring constant Δk are constant, and the x'- and y'-axes rotate with a constant angular velocity ω. But as shown by Fig. 1. 12, for the experimental apparatus, the mean value of the natural frequencies p_m and

the difference of them p_d do not take constant values for changes in θ, hence the spring constant k and the difference Δk are not constant. Consequently, (1) when the shaft rotates, k and Δk fluctuate periodically with frequencies ω, 2ω, ... around the average values k and $\overline{\Delta k}$. Furthermore, since α deviates from the broken line by about 15°~20°, as shown in Fig. 1. 11. (2) when the shaft rotates with an angular velocity ω, the x'- and y'-directions rotate with the average angular velocity ω. experiencing a periodic angular acceleration. Coexistence of the anisotropy fixed in space and the rotating anisotropy results in a change of the static deflection of the shaft. Thus, (3) periodic disturbing forces with frequencies 2ω, 3ω, ..., as well as ω, are exerted on the shaft[6]. From (1) and (2) mentioned above, terms of parametric excitation, terms representing the fixed anisotropy of stiffness, and terms of rotating anisotropies rotating with $\pm n\omega$ (n is an integer) are derived. However, it can be concluded through analysis that if we confine the problem to forced vibrations of frequency ω, and if we reject all but linear terms of small quantities, the derived terms caused by (1) and (2), and the disturbing forces of higher frequencies mentioned in (3) have no connection with our discussions. It follows that only the terms containing $\bar{k}$ and $\overline{\Delta k}$, i. e., the average values of k and Δk, are concerned with our discussions. Obviously, $\bar{k}$ and $\overline{\Delta k}$ correspond to $\bar{p}_m$ and $\bar{p}_d$, the average values of p_m and p_d.

We obtained spring characteristics between the moment and the inclination angle of the disc, as shown in Fig. 1. 13. In the figure, we can see that there also exist spring characteristics represented by cubes of the coordinates. Since experiments were performed in the range $-0.4° \sim +0.4°$ of inclination angle (Fig. 1. 13), the system can be considered approximately as one having unsymmetrical nonlinear characteristics represented by the second power of the coordinates.

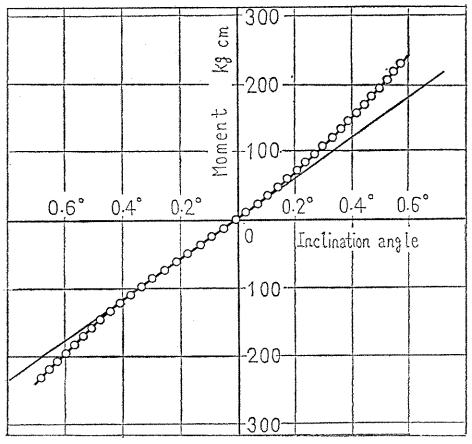

Fig. 1. 13. Spring characteristics

From the experimental results shown in Figs. 1. 11, 1. 12, and 1. 13, it is seen that if $\bar{k}$ and $\overline{\Delta k}$ are replaced by k and Δk, the spring characteristics of our experimental apparatus can be represented by Eq. (1. 3), which have anisotropies of stiffness and of unsymmetrical nonlinearity rotating with ω. Accordingly, the analytical results obtained in the preceding section can be applied to our experiments, in so far as we consider harmonic oscillations of frequency ω.

The spring characteristics represented by Figs. 1. 11~1. 13 result in the resonance curves shown in Figs. 1. 14~1. 17, depending on whether the eccentricity of the rotor is located in quadrant Ⅰ, Ⅱ, Ⅲ, or Ⅳ, respectively. Since $\varepsilon_x' > 0$ and $\varepsilon_y' < 0$ hold in our experimental apparatus, Figs. 1. 14, 1. 15, 1. 16, and 1. 17 correspond to Figs. 1. 2, 1. 3, 1. 4, and 1. 5, respectively. In Figs. 1. 14, 1. 15, and 1. 16, as well as in Figs. 1. 2, 1. 3, and 1. 4, there exist unstable regions. In Fig. 1. 17, there exists no unstable region, similar to the one in Fig. 1. 5. In Fig. 1. 17, jump phenomena,

indicated by arrows, take place. Similar to Fig. 1. 3, the unstable region is the widest in Fig. 1. 15 and has the range of about $1120 \sim 1500$ rpm. The calculated value for the major critical speed ω_c in our experimental apparatus is about 1121. 3 rpm when the shaft is supported freely at both ends, and it increases to about 2420. 8rpm when it is supported freely at the upper end and fixed at the lower end. Accordingly, the unstable region has a width of about $2420.8-1121.3 \simeq 1300$rpm at its maximum, but in Fig. 1. 15 its width is about 380rpm, which is about 29% of the maximum value. In Fig. 1. 14, as in Fig. 1. 2, the unstable region becomes narrower from the higher speed side, and in Fig. 1. 16, it becomes narrower from the lower

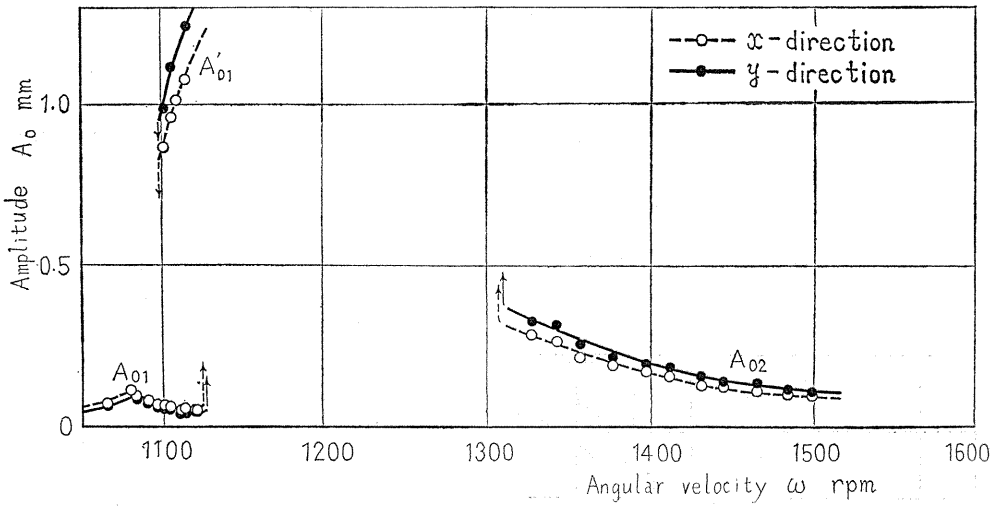

Fig. 1. 14. Resonance curve (corresponds to Fig. 1. 2., US-type, $\varepsilon'_x>0$, $\varepsilon'_y<0$, eccentricity is located in quadrant I)

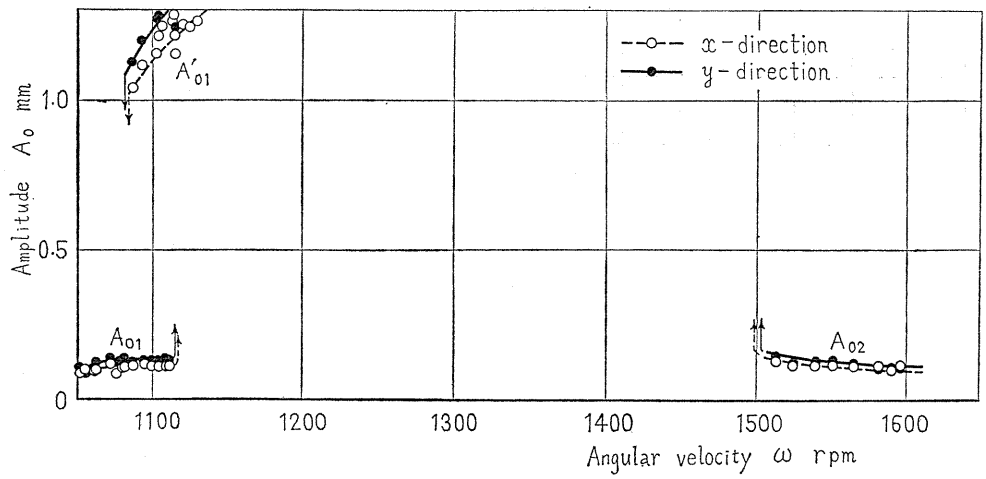

Fig. 1. 15. Resonance curve (corresponds to Fig. 1. 3, UU-type, $\varepsilon'_x>0$, $\varepsilon'_y<0$, eccentricity is located in quadrant II)

speed side in the same way as in Fig. 1. 4. As we see from Figs. 1. 14～1. 17, A_{02} of the lower speed side and A_{01} of the higher speed side did not appear in our experiments. The large amplitude resonance curves A'_{01} of the lower speed side in Figs. 1. 14 and 1. 15 are not curves corresponding to A_{02} of the lower speed side in Figs. 1. 2 and 1. 3, but are curves caused by the influence of the symmetrical

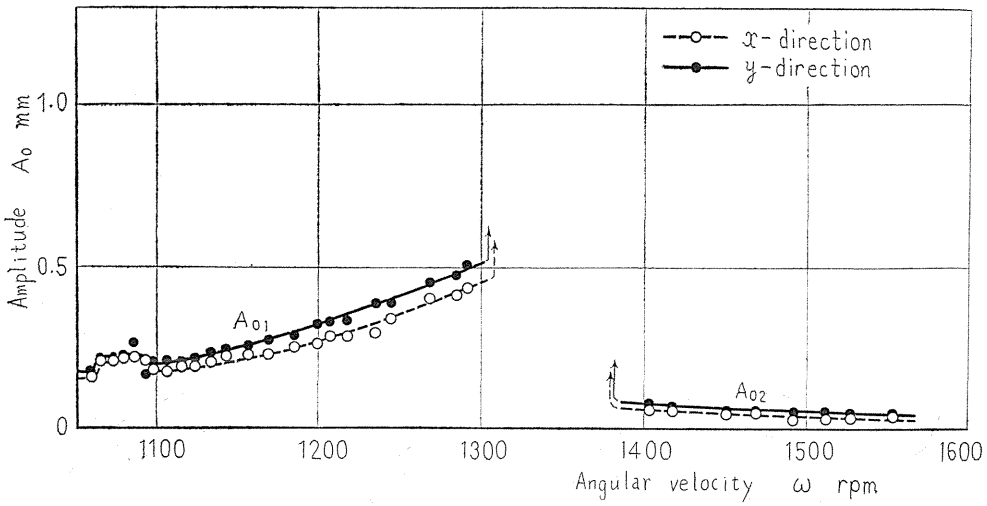

Fig. 1. 16. Resonace curve (corresponds to Fig. 1. 4, SU-type, $\varepsilon'_x>0$, $\varepsilon'_y<0$, eccentricity is located in quadrant Ⅲ)

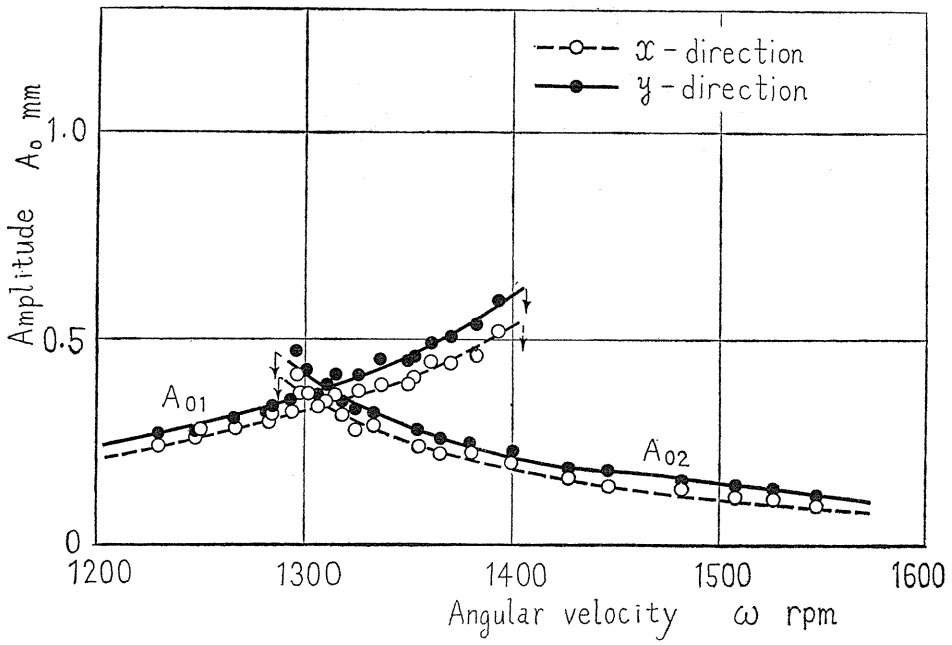

Fig. 1. 17. Resonance curve (corresponds to Fig. 1. 5, SS-type, $\varepsilon'_x>0$, $\varepsilon'_y<0$, eccentricity is located in quadrant Ⅳ)

nonlinearity of the spring characteristics. It can be said that the experimental results in Figs. 1. 14~1. 17 agree with the analytical results obtained in the preceding section.

In many experiments performed in the same spring conditions as in Figs. 1. 11~1. 17, we measured the amplitude A_0 and the angle δ between the top of the vibratory wave and the rotation mark P for vibratory waves obtained at a lower rotating speed than the major critical speed ω_c. The results are shown in Fig. 1. 18 (a) where the polar coordinates (A_0, δ) are adopted. For the U-type in which the resonance curve A_{01} of the lower speed side does not extend to the higher speed side (Figs. 1. 14 and 1. 15), the symbol △ is used, and for the S-type in which A_{01} extends to the higher speed side (Figs. 1. 16 and 1.17), the symbol ○ is used. After a number of experiments, it can be seen that symbols △ (the U-type) gather in quadrants Ⅰ and Ⅱ, and symbols ○ (the S-type) gather in quadrants Ⅲ and Ⅳ, as shown in Fig. 1. 18 (a). Similarly, for the vibrations of the higher speed side than ω_c, the symbol △ is used for an A_{02}-curve of the U-type which does not extend to the lower speed side (Figs. 1. 15 and 1. 16); the symbol ○ is adopted for that of the S-type which extends to the lower speed side (Figs. 1. 14 and 1.17). In this way

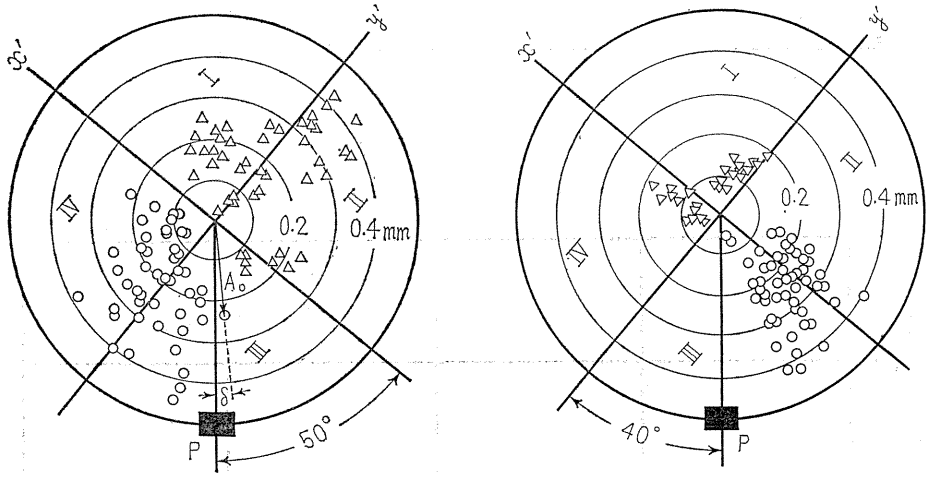

(a) $\omega<\omega_c$ (b) $\omega>\omega_c$

Fig. 1. 18. Polar coordinates (A_0, δ)
$(\varepsilon'_x>0, \varepsilon'_y<0$, △ : U-type, ○ : S-type)

Fig. 1. 18 (b) is obtained, where the symbols ○ and △ gather in quadrants Ⅱ, Ⅲ, and quadrants Ⅰ, Ⅳ, respectively. If the magnification factors of a_0 and b_0 in the preceding section are equal, the angular position of the top of the vibratory wave coincides with the direction of the eccentricity when $\omega<\omega_c$, and it differs by 180° when $\omega>\omega_c$. Since in experiments, the magnification factors of a_0 and b_0 are generally not equal, the angular position of the top of the vibratory wave does not agree with the direction of the eccentricity. It can be concluded, however, that the direction of the top of a vibratory wave is always located in the quadrant in which the eccentricity exists. Consequently, Figs. 1. 18 (a) and 1. 18 (b) prove experimentally that when the eccentricity is located in quadrants Ⅰ, Ⅱ, Ⅲ, and Ⅳ, the

resonance curves take the shapes of Fig. 1. 2 (Fig. 1. 14), Fig. 1. 3 (Fig. 1. 15), Fig. 1. 4 (Fig. 1. 16), and Fig. 1. 5 (Fig. 1. 17), respectively.

Depending on small differences in the assembling conditions, the values of the anisotropy of shaft stiffness Δk and of the coefficients ε'_x and ε'_y of nonlinear terms vary. When the values of Δk, ε'_x and ε'_y become smaller then those of Figs. 1. 11～1. 18, the resonance curves for an eccentricity located in quadrant Ⅳ become as shown in Fig. 1. 19. Though the resonance curves become steeper, they are qualytatively the same as those of Figs. 1. 5 and 1. 17.

When certain conditions are met in the assembled apparatus, ε'_x vanishes and the nonlinearity appears only in the y'-direction, where the stiffness is $k-\Delta k$, as shown

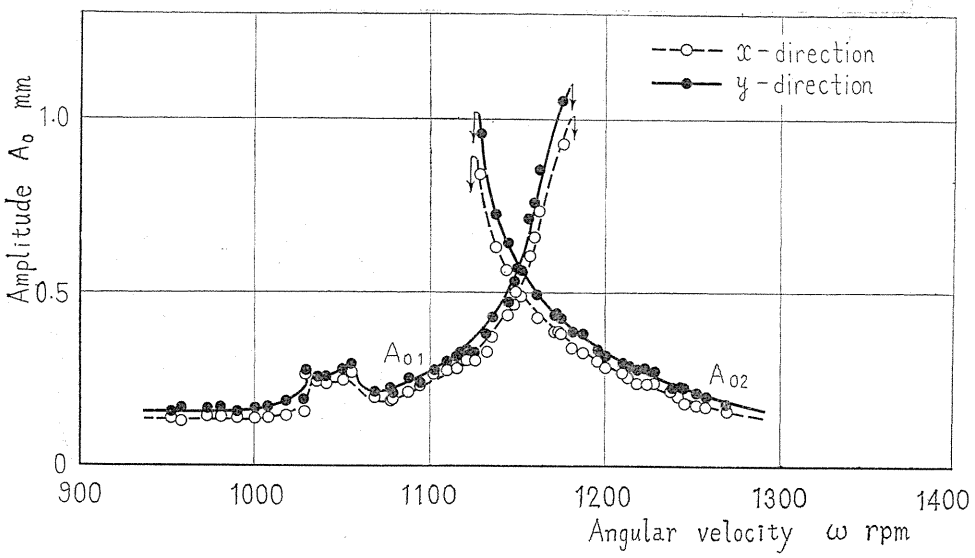

Fig. 1. 19. Resonance curve (corresponds to Fig. 1. 5. and Fig. 1. 17)

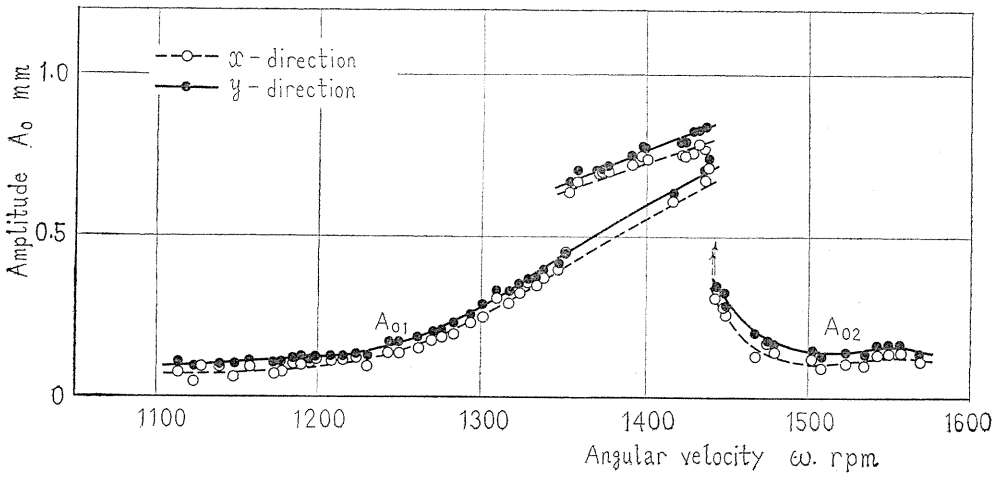

Fig. 1. 20. Resonance curve (corresponds to Fig. 1. 7. $\varepsilon'_x \fallingdotseq 0$, $\varepsilon'_y > 0$)

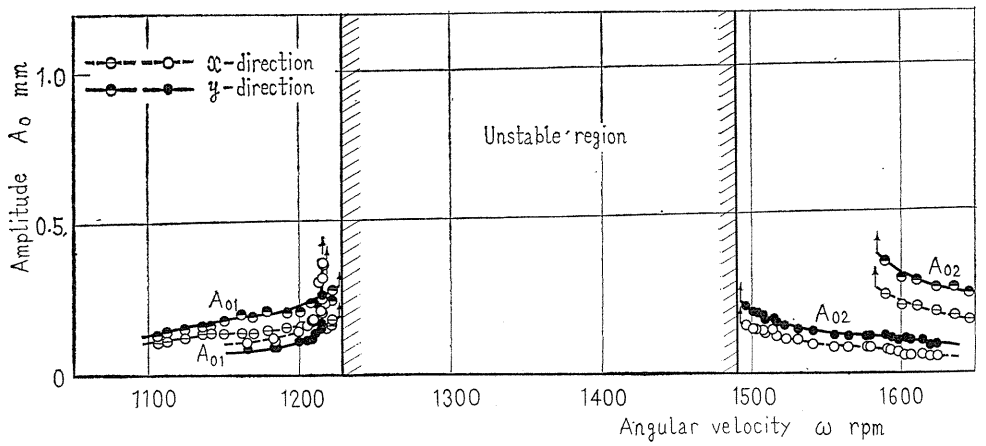

Fig. 1. 21. Resonance curve (corresponds to Fig. 1. 8. $\varepsilon'_x \neq 0$, $\varepsilon'_y > 0$)

in Figs.1. 7 and 1. 8. Experimental results for the resonance curves in such a case are shown in Figs. 1. 20 and 1. 21, and they are similar to the analytical results shown in Figs. 1.7 and 1. 8, respectively. The double resonance curves in Fig. 1. 20 appeared because the magnitude and the location of the eccentricity varied a little when we experimented later to supplement our experimental data. As shown in Fig. 1. 21, we could not ascertain the existence of the stable region b~c in Fig. 1. 8, because it was dangerous to experiment in this range. In Fig. 1. 22, the relation between the direction of the top of a vibratory wave and the shape of the resonance curve for the lower speed side is shown. This figure was obtained through a number of experiments. For the type of Fig. 1. 20 (Fig. 1. 7) the symbol ○ is used. and for the type of Fig. 1. 21 (Fig. 1. 8) the symbol △ is employed. The symbol ○ and △ are divided by the x'-axis into quadrants Ⅰ, Ⅱ ($\beta \simeq 0° \sim 180°$) and quadrants Ⅲ, Ⅳ ($\beta \simeq 180° \sim 360°$). This fact obviously agrees with the conclusions obtained analytically in the preceding section.

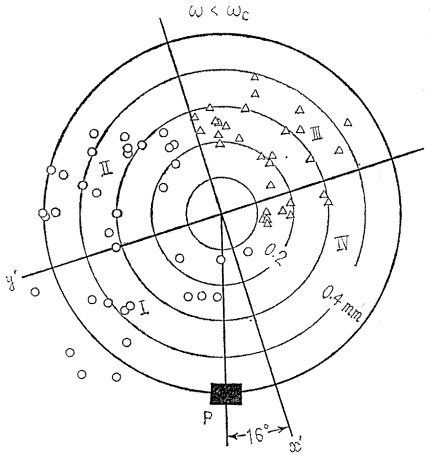

Fig. 1. 22. Polar coordinates (A_0, δ), ($\varepsilon'_x \neq 0$, $\varepsilon'_y > 0$, △ : U-type, ○ : S-type)

1. 5. Conclusions

Particular vibration phenomena caused by ball bearings in the neighborhood of the major critical speed are treated in the present chapter.

(1) When a rotating shaft is supported by single-row deep groove ball bearings, the anisotropies of shaft stiffness and of unsymmetrical nonlinearity rotating with the shaft appear in the spring characteristics, caused by (a)~(d), as noted in section 1. 1.

(2) In such a system, unstable regions appear and disappear, and various shapes of resonance curves can be observed, both as a function of the angular position of the eccentricity of the rotor.

(3) When nonlinearities exist in both directions of the maximum and minimum stiffnesses, four kinds of resonance curves appear depending on the angular position of eccentricity.

(4) When a nonlinearity does not exist in the direction of the maximum stiffness, resonance curves are classified into two kinds.

(5) Such particular vibration phenomena, that is, the appearance and the disappearance of unstable regions and variations in the shapes of resonance curves, caused by the angular position of eccentricity, can be explained by considering the rotating anisotropy of stiffness rotating with the shaft and the anisotropy of unsymmetrical nonlinear spring characteristics, represented by the second power of coordinates, which also rotates with the shaft.

Chapter II. Oscillations of a Rotating Shaft with Symmetrical Nonlinear Spring Characteristics[8]

2. 1. Introduction

When a single-row deep groove ball bearing is used in a rotating shaft system, the equilibrium position of a shaft center line deviates from the center of the "angular clearance[2]" of the ball bearing provided that the center lines of both bearing pedestals are not in alignment. Accordingly, unsymmetrical nonlinear characteristics (represented by even order terms in the polynominals for the restoring forces) appear more strongly than symmetrical nonlinear characteristics (represented by odd order terms) in the restoring forces of the shaft. Whirling oscillations such as subharmonic oscillations of order 1/2, summed-and-differential harmonic oscillations of the type $[p_i \pm p_j]$, etc., take place in such a system. One of the authors has already reported experimental[2),(4),(5)] and theoretical[9),(10)] researches on them. Since the directional nonuniformity of shaft stiffness (the nonuniformity of linear terms in the polinominals representing restoring forces for different directions) and unsymmetrical nonlinear characteristics appear simultaneously, forced oscillations of synchronous backward precession take place concurrently with nonlinear forced oscillations. These oscillations have been also reported by one of the authors[3].

Through our experiments, it can be pointed out that unsymmetrical nonlinear characteristics are likely to appear more strongly than symmetrical ones when a single-row deep groove ball bearing is employed. However, if a vertical shaft system is assembled carefully to align both center lines of the upper and lower bearing pedestals, the shaft center line is located at the center of the angular clearance. Hence symmetrical nonlinear characteristics appear more strongly than unsymmetrical ones.

In this chapter, it is shown experimentally that various whirling motions due to symmetrical nonlinear characteristics, i. e. subharmonic oscillations of order 1/3 and summed-and-differential harmonic oscillations of the types $[2p_i \pm p_j]$ and $[p_i \pm p_j \pm p_k]$, take place in a rotating shaft system whose bearing pedestals are aligned fairly well. These oscillations have not been reported in the previous papers[2),(4),(5)]. There are some reports[11)~(15)] by one of the authors and other researchers about

various forced oscillations due to symmetrical nonlinear characteristics in rectilinear systems, but there exists no report about such oscillations of whirling motion in a rotating shaft system. Furthermore, it is pointed out in this chapter that the existence of somewhat strong symmetrical nonlinear characteristics results in the followings: The resonance curves in the neighborhoods of the major critical speeds and those for forced oscillations of synchronous backward precession become those of the hard spring type with jump phenomena, which have not been reported in the previous papers[3]. The resonance curves of subharmonic oscillations of order 1/2 and of summed-and-differential harmonic oscillations of the type $[p_i \pm p_j]$, which are caused by unsymmetrical nonlinear characteristics, are bent more strongly toward the higher speed side than those in the previous papers[2],[4],[5]. This is due to the existence of strong symmetrical nonlinear characteristics. Among these unsymmetrical nonlinear forced oscillations, those being less frequent in occurrence appear only in the system[2],[4],[5] with strong unsymmetrical nonlinear characteristics and do not appear in the system of this chapter with weak unsymmetrical ones.

The different representation of nonlinear spring characteristics from those of a rectilinear system should be adopted for the theoretical analysis of nonlinear forced oscillations of a rotating shaft, because they are whirling motions in the xy-plane (Fig. 1.10). A detailed theoretical analysis will be shown in the next chapter. The experimental results of this chapter can be explained by using the theoretical results of Chapter Ⅲ.

2. 2. Experimental apparatus and oscillations expected to occur

The experimental apparatus is the same as those used in the previous chapter (Fig. 1.10). The dimensions of the experimental apparatus are the same, but the assembling condition is different.

For the natural frequencies of the rotating shaft system shown in Fig. 1.10, the following relationships always hold[16].

(i) The system has the four natural frequencies p_i (i=1∼4), and the relationship

$$p_1 > p_2 > 0 > p_3 > p_4 \tag{2.1}$$

always holds. p_1, p_2 and p_3, p_4 are natural frequencies of modes of forward and backward precessions, respectively.

(ii) The natural frequency p_1 has the relationships:

$$p_1 > (I_p/I)\cdot\omega, \quad \lim_{\omega\to\infty} p_1 = (I_p/I)\cdot\omega \tag{2.2}$$

(iii) The frequencies p_2, p_3, and p_4 approach certain finite values when $\omega\to\infty$, and they never become infinite in the whole range of $\omega=0\sim\infty$.

In Fig. 2.1, the magnitudes of $p_1\sim p_4$ of our experimental apparatus are represented against the angular velocity ω by solid lines. Some of the absolute values of summations and differences of frequencies, which are necessary for the later discussions, are also illustrated by broken lines.

Among various forced oscillations which are caused by symmetrical nonlinear characteristics expressed by odd power terms of coordinates, those due to higher order terms rarely appear. So the terms higher than the third power are negrected. In the neighborhoods of ω where the relationships

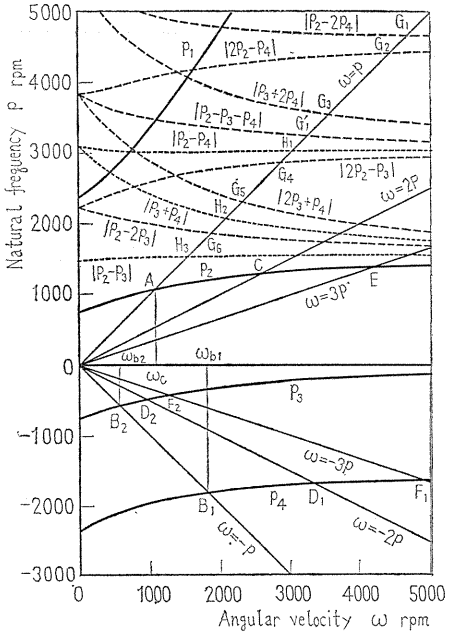

Fig. 2. 1. $p-\omega$ diagram

$$\omega=3p_1, \quad \omega=3p_2, \quad \omega=-3p_3, \quad \text{and} \quad \omega=-3p_4 \tag{2.3}$$

hold, the subharmonic oscillations with the frequencies

$$\omega_1=1/3\cdot\omega, \quad \omega_2=1/3\cdot\omega, \quad \omega_3=-1/3\cdot\omega, \quad \text{and} \quad \omega_4=-1/3\cdot\omega, \tag{2.4}$$

appear, respectively. In the neighborhoods of ω given by

$$\omega=|2p_i\pm p_j| \quad (i\neq j,\ i,\ j=1,\ 2,\ 3,\ 4), \tag{2.5}$$

the summed-and-differential harmonic oscillations take place, i. e., two oscillations of the frequencies ω_i and ω_j having the relationships

$$\omega_i\fallingdotseq p_i, \quad \omega_j\fallingdotseq p_j, \quad \omega=|2\omega_i\pm\omega_j| \tag{2.6}$$

appear simultaneously. And in the neighborhoods of

$$\omega=|p_i\pm p_j\pm p_k| \quad (i\neq j\neq k,\ i,\ j,\ k=1,\ 2,\ 3,\ 4), \tag{2.7}$$

the summed-and-differential harmonic oscillations consisting of three oscillations of the frequencies ω_i, ω_j, and ω_k having the relationships

$$\omega_j\fallingdotseq p_i, \quad \omega_j\fallingdotseq p_j, \quad \omega_k\fallingdotseq p_k, \quad \omega=|\omega_i\pm\omega_j\pm\omega_k| \tag{2.8}$$

appear.

The relationship $p_1>2\omega$ is derived from (ii) because $I_p/I\fallingdotseq 2$ holds in our experimental apparatus. It is easily seen from this and (iii) that there is no angular

velocity ω which satisfies Eqs. (2.3), (2.5), and (2.7) containing p_1. And similarly to the case of a rectilinear system[13),(15)], it can be proved that, among summed-and-differential harmonic oscillations of whirling motion, only those of the summed type respecting absolute values of natural frequencies can take place in a rotating shaft system. Consequently, subharmonic and summed-and-differential harmonic oscillations which are expected to occur in our experimental apparatus are limited to those which satisfy the relationships:

$$\omega=3p_2,\quad \omega=-3p_3,\quad \omega=-3p_4, \tag{2.9}$$

$$\left.\begin{aligned}&\omega=p_2-2p_4,\quad \omega=2p_2-p_4,\quad \omega=-p_3-2p_4,\\&\omega=2p_2-p_3,\quad \omega=-2p_3-p_4,\quad \omega=p_2-2p_3,\end{aligned}\right\} \tag{2.10—a}$$

$$\omega=p_2-p_3-p_4. \tag{2.10—b}$$

The angular velocities where these oscillations appear are indicated by the abscissas of the intersection points E, F_2, F_1, $G_1\sim G_6$, and G_1' in Fig. 2.1. We represent these angular velocities by the symbols $\omega_{\frac{1}{3}}$, $\omega'_{-\frac{1}{3}}$, $\omega_{-\frac{1}{3}}$, ω_{244}, ω_{224}, ω_{344}, ω_{223}, ω_{334}, ω_{233}, and ω_{234}, respectively.

Most forced oscillations due to unsymmetrical nonlinear characteristics are caused by the second power terms of coordinates. Among these oscillations, those which are expected to occur are limited to those which satisfy the relationships:

$$\omega=2p_2,\quad \omega=-2p_3,\quad \omega=-2p_4, \tag{2.11}$$

$$\omega=p_2-p_4,\quad \omega=-p_3-p_4,\quad \omega=p_2-p_3, \tag{2.12}$$

for the same reason as before. The angular velocities where these oscillations occur are given by C, D_2, D_1, and $H_1\sim H_3$ in Fig. 2. 1. We represent these by $\omega_{\frac{1}{2}}$, $\omega_{-\frac{1}{2}}'$, $\omega_{-\frac{1}{2}}$, ω_{24}, ω_{34}, and ω_{23}.

2. 3. Experimental results

(I) *Spring characteristics*

The experimental apparatus was assembled carefully to attain good alignment of center lines of the upper and the lower bearing pedestals. Its spring characteristics are shown in Figs. 2. 2 and 2. 3.

In Fig. 2. 2, it was examined whether the rotating directional nonuniformity of shaft stiffness exists as in the previous paper[1] or not. When $\omega=0$, the natural frequencies p_{01} and p_{02} in the directions of the maximum and minimum stiffnesses, respectively, are measured for various angular position θ (Fig. 1. 10) of the rotor.

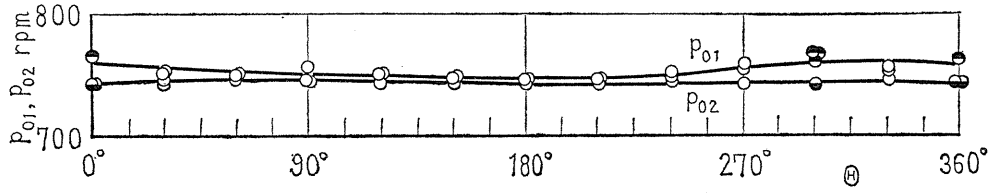

Fig. 2. 2. Natural frequencies when $\omega=0$

The former and the latter are indicated by the symbols ◓ and ◒, respectively, and the frequencies which can not be distinguished are shown by the symbols ○. From this figure, it is found that the difference between p_{01} and p_{02} is little and does not change with θ. Accordingly it can be concluded that the rotating difference of shaft stiffness does not exist.

The relationships between the moment exerted on the disk and the inclination angle of the disk for various directions denoted by φ are shown in Fig. 2. 3, when the angular position of the disk is kept at $\theta=0$. In opposition to Fig. 5 in the previous paper[2], symmetrical nonlinear characteristics appear more strongly than unsymmetrical nonlinear characteristics. Since all the characteristic curve in Fig. 2. 3 take a similar shape, it can be seen that this symmetrical nonlinear restoring force characteristics are directionally uniform (isotropic).

Spring characteristics shown in Fig. 2. 4 which were measured after the reassembly differ a little from those in Figs. 2. 2 and 2. 3. Symmetrical nonlinear characteristics still appear strongly in Fig. 2. 4, but the shape of characteristic curve changes with the direction φ, that is, they are directionally nonuniform (anisotropic). In other words, when the restoring force characteristics, for example, in the x- and y-directions are represented by $\alpha x+\beta_x x^3$ and $\alpha y+\beta_y y^3$, respectively, the coefficients β_x and β_y are equal in Fig. 2. 3 and unequal in Fig. 2. 4.

Figure 2. 3 and 2. 4 show the characteristic curves of hard spring type. This is understood because nonlinear characteristics are caused by the angular clearance of the single-row deep groove ball bearing.

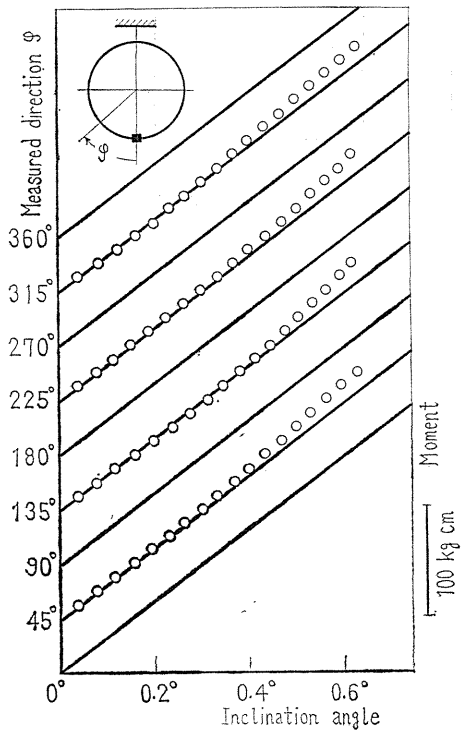

Fig. 2.3. Spring characteristics (I)

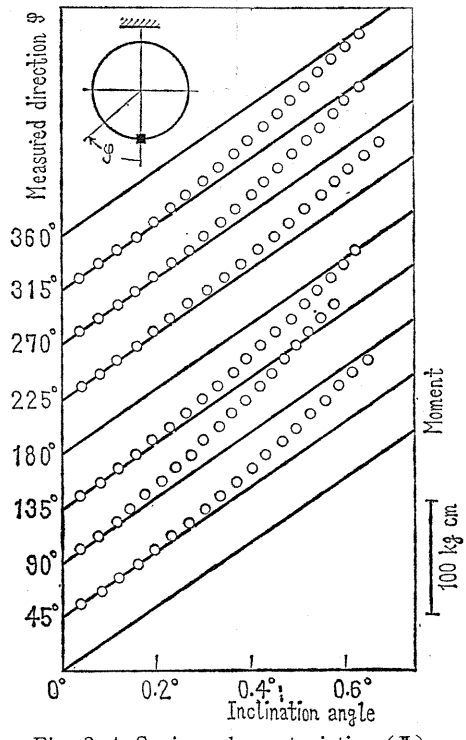

Fig. 2. 4. Spring characteristics (II)

(Ⅱ) *Forced oscillations of whirling motion which are influenced by symmetrical nonlinear characteristics*

(Ⅱ-*a*) *Oscillations whose shapes of resonance curves are influenced*

Among the oscillations occurring in the system with characteristics shown in Fig. 2. 3, only those related to symmetrical nonlinear characteristics are shown in Fig. 2. 5. The oscillations in the neighborhoods of ω_{b2}, ω_c, and ω_{b1} (Fig. 2. 1) can occur also in the linear systems.

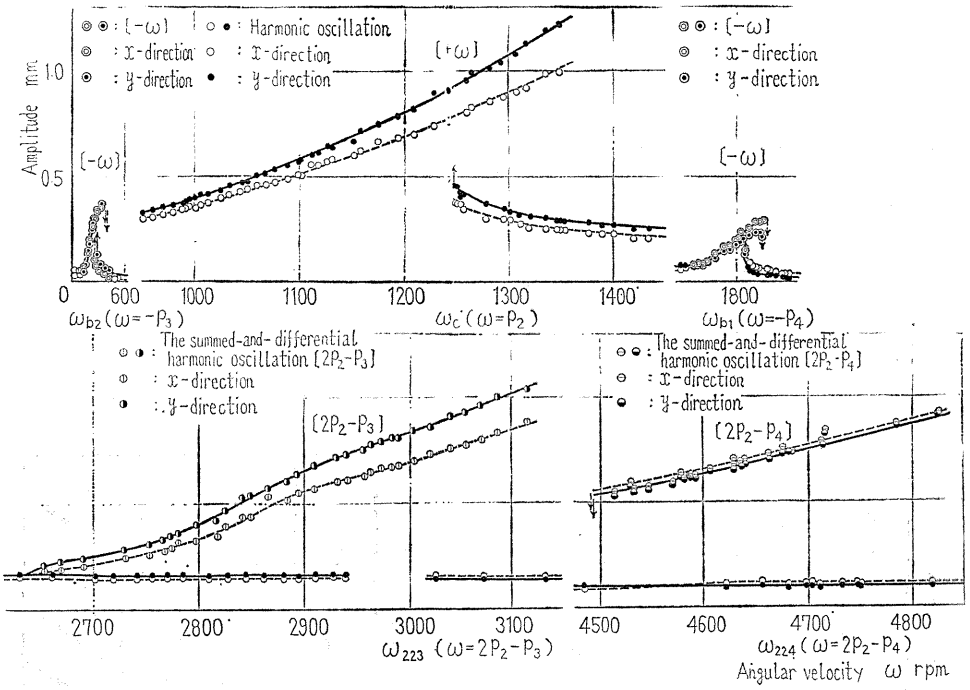

Fig. 2. 5. Oscillations occurred in a system with isotropic symmetrical nonlinear spring characteristics

The oscillation in the neighborhood of the major critical speed ω_c where $\omega=p_2$ holds has a typical resonance curve of a hard spring type, because of symmetrical nonlinear characteristics. It was accompanied by a jump and a hysteresis phenomena like that of rectilinear systems. Though the upper branch of the resonance curve extends further to the higher speed region, the experiment was stopped at about 1350rpm for safety. Hereafter, if the upper branch of a resonance curve ends with no arrow indicating jump at its highest edge, it implies that the experiment is stopped for the same reason.

In the neighborhoods of ω_{b2} and ω_{b1}, where $\omega=-p_3$ and $\omega=-p_4$ hold, respectively, forced oscillations of synchronous backward precession of the frequency $-\omega$ appear due to the directional nonuniformity of shaft stiffness. Their amplitudes are proportional to this difference[17], which is caused by the directional nonuniformity of stiffness of pedestals[17] and by unsymmetrical nonlinear characteristics due to

angular clearances of ball bearings[3]. Therefore, comparing with the previous paper[3] for a system where unsymmetrical nonlinear characteristics appeared strongly, the amplitudes of such oscillations in Fig. 2. 5 are considerably small because the unsymmetrical nonlinear characteristics appear weakly in this case. The shape of the resonance curves in the paper[3] were the same as those of a linear system because symmetrical nonlinear characteristics were weak, but those in this chapter take the shape of a hard spring type because they are strong. It is similar to the case of the major critical speed.

In the case of Fig. 2. 4 having anisotropic nonlinear characteristics, almost the same results as those in Fig. 2. 5 are obtained for ω_c, ω_{b1}, and ω_{b2}.

(Ⅱ-*b*) *Oscillations whose occurrence is influenced*

In Fig. 2. 5, the summed-and-differential harmonic oscillations in the neighborhoods of ω_{223} and ω_{224}, where $\omega=2p_2-p_3$ and $\omega=2p_2-p_4$ hold, respectively, do not appear if there is no symmetrical nonlinear characteristics.

In the neighborhood of ω_{223} in Fig. 2. 5, two oscillations of forward and backward precessions, whose frequencies are ω_2 $(\simeq p_2)$ and ω_3 $(\simeq p_3)$, respectively, occur simultaneously in the wide range of $\omega>2640$rpm.

The frequencies ω_2 and ω_3 of the summed-and-differential harmonic oscillation $[2p_2-p_3]$ are shown in Fig. 2. 6. The points representing the values of ω_2 $(\simeq p_2)$ and $\omega_3(\simeq p_3)$ obtained in experiments are almost on two straight lines passing through the origin.

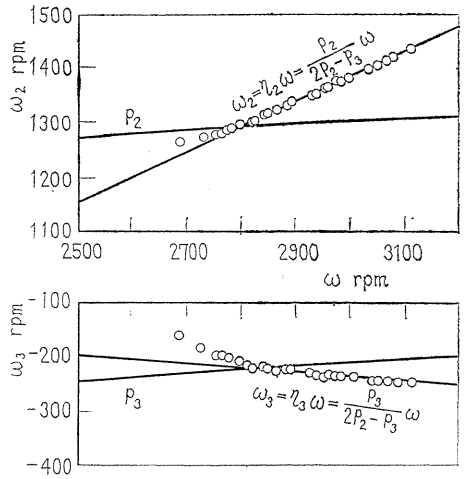

Fig. 2. 6. Frequencies of the summed-and-differential harmonic oscillation of the type $[2p_2-p_3]$

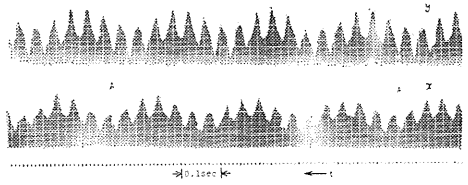

$\omega=3000$rpm, $\omega:\omega_2:\omega_3=37:17:(-3)$

Fig. 2. 7. Waves of the summed-and-differential harmonic oscillation of the type $[2p_2-p_3]$

The vibratory waves of the oscillation of the type $[2p_2-p_3]$ are shown in Fig. 2. 7, White vertical lines in the figure are rotation marks recorded at each rotation of the shaft by using the small paper P shown in Fig. 1. 10. The superimposed oscillation of a small amplitude is the harmonic component of the frequency ω, and it appears in all the vibratory waves shown in this paper. The waves have a period

corresponding to the distance between two points marked A. In the interval AA, the shaft rotates 37 times, the rapid oscillation swings 17 times, and the slow oscillation swings 3 times. Furthermore, from the comparison of the phases in the x- and y-directions, it can be seen that the rapid one is a forward precession and the slow one is a backward precession. We represent a forward precession by the sign plus and a backward precession by the sign minus. Thus we find $\omega:\omega_2:\omega_3=37:17:(-3)$ aud $\omega=2\omega_2-\omega_3$.

In the neighborhood of ω_{224} in Fig. 2. 5, the summed-and-differential harmonic oscillations $[2p_2-p_4]$ occur in the range of $\omega>4500$rpm. The frequencies ω_2 and ω_4 are shown in Fig. 2. 8, which are almost on two straight lines passing through the origin. The vibratory waves are shown in Fig. 2. 9 where $\omega:\omega_2:\omega_4=16:5:(-6)$ and $\omega=2\omega_2-\omega_4$ hold.

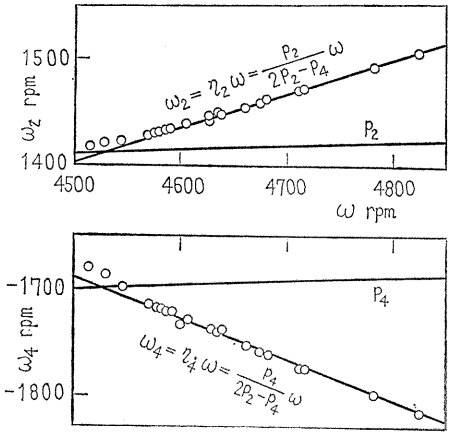

Fig. 2. 8. Frequencies of the summed-and-dfferential harmonic oscillation of the type $[2p_2-p_4]$

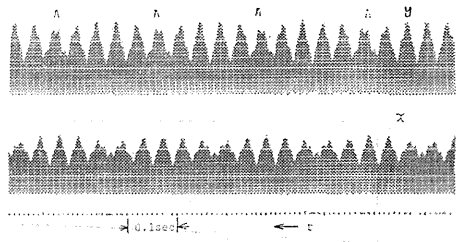

$\omega=4582$rpm, $\omega:\omega_2:\omega_4=16:5:(-6)$

Fig. 2. 9. Waves of the summed-and-differential harmonic oscillation of the type $[2p_2-p_4]$

The shapes of both oscillations of the types $[2p_2-p_3]$ and $[2p_2-p_4]$ are those of a hard spring type, as seen in Fig. 2. 5.

In the range of $\omega>2600$rpm in Fig. 2. 5, small harmonic oscillation of frequency ω (symbol ○ ●) appear as well as summed-and-differential harmonic oscillation (symbol ⓘ ◑). Which of the two will take place depends on the initial conditions.

The above-mentioned nonlinear forced oscillations are obtained in the system having the isotropic symmetrical nonlinear characteristics shown in Fig. 2. 3. In the system with anisotropic symmetrical nonlinear characteristics of Fig. 2. 4, the following oscillations occur in addition to the oscillations of the types $[2p_2-p_3]$ and $[2p_2-p_4]$ shown in Fig. 2. 5: The subharmonic oscillation of order 1/3 of the type $[3p_2]$, the summed-and-differential harmonic oscillations of the types $[p_2-2p_3]$ and $[p_2-2p_4]$, and the summed-and-differential harmonic oscillation of the type $[p_2-p_3-p_4]$ in which three oscillations appear simultaneously. These oscillations shown in Fig. 2. 10 are due to anisotropic symmetrical nonlinear characteristics, and all the resonance curves are those of a hard spring type.

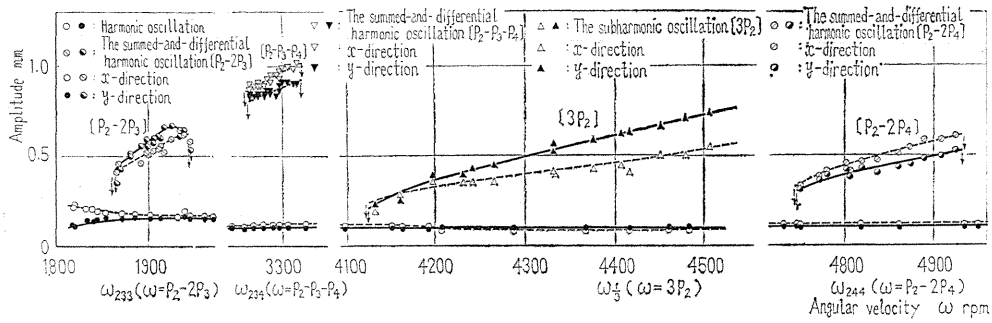

Fig. 2. 10. Oscillations occurring only in a system with anisotropic symmetrical nonlinear spring characteristics

In the neighborhoods of the angular velocities ω_{233} and ω_{244}, where $\omega=p_2-2p_3$ and $\omega=p_2-2p_4$ hold, respectively, the summed-and-differential harmonic oscillations of the types $[p_2-2p_3]$ and $[p_2-2p_4]$ occur. The former appears in the range of $\omega\simeq$1860~1940rpm, the latter in the range of $\omega\simeq$4750~4930rpm, and these ranges are comparatively narrow. The frequencies of these oscillations are shown in Figs. 2. 11 and 2. 12, which are almost on two straight lines passing through the origin. The vibratory waves are shown in Figs. 2. 13 and 2. 14, where we find the relationships $\omega:\omega_2:\omega_3=40:26:(-7)$, $\omega=\omega_2-2\omega_3$ and $\omega:\omega_2:\omega_4=54:16:(-19)$, $\omega=\omega_2-2\omega_4$.

The summed-and-differential harmonic oscillation of the type $[p_2-p_3-p_4]$ shown in Fig. 2. 10 occur in the neighborhood of the angular velocity ω_{234} where $\omega=p_2-p_3-p_4$ holds. It consists of three oscillations with the frequencies ω_2 $(\simeq p_2)$, ω_3 $(\simeq p_3)$, and ω_4 $(\simeq p_4)$. This oscillation appears in somewhat narrow range of $\omega\simeq$3265~3320rpm. Its frequencies and vibratory waves are shown in Figs. 2. 15 and 2. 16, respectively. Their general features are similar to those of a recti-

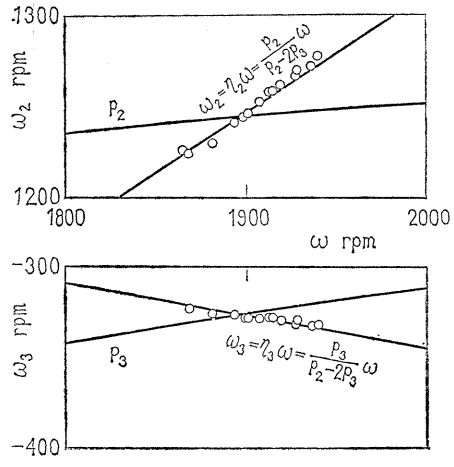

Fig. 2. 11. Frequencies of the summed-and-differential harmonic oscillation of the type $[p_2-2p_3]$

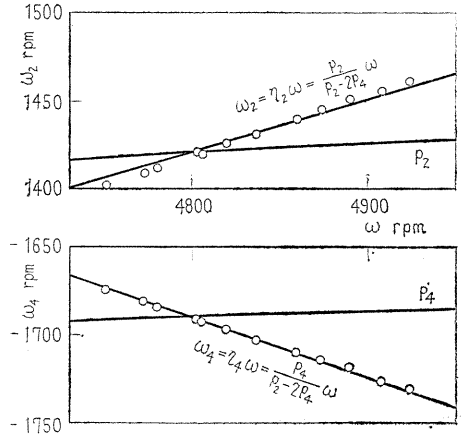

Fig. 2. 12. Frequencies of the summed-and-differential harmonic oscillation of the type $[p_2-2p_4]$

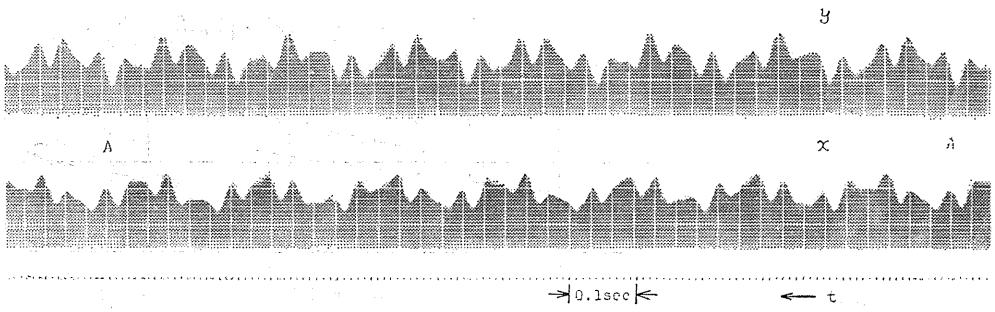

ω=1878rpm, $\omega : \omega_2 : \omega_3$=40 : 26 : (−7)

Fig. 2. 13. Waves of the summed-and-differential harmonic oscillation of the type $[p_2-2p_3]$

linear system reported in the paper[15]. In the interval AA in Fig. 2. 16, the long wave with the frequency ω_3 oscillates 7 times in a backward precession, the short wave of the frequency ω_2 with large amplitude oscillates 43 tims, and it can be found from the beating change of the wave with the frequency ω_2 that the

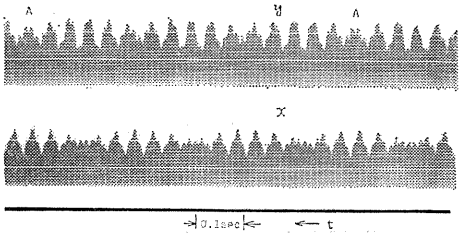

ω=4860rpm, $\omega : \omega_2 : \omega_4$=54 : 16 : (−19)

Fig. 2. 14. Waves of the summed-and-differential harmonic oscillation of the type $[p_2-2p_4]$

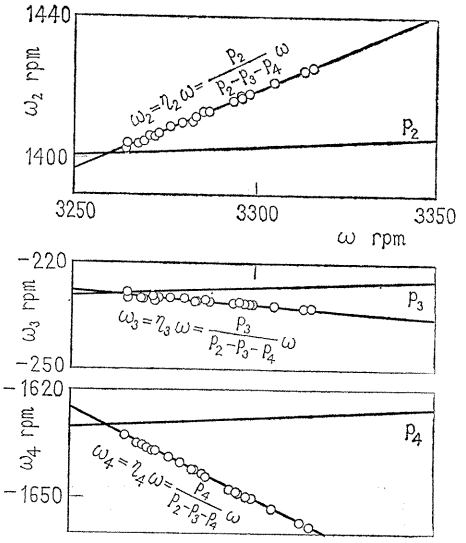

Fig. 2. 15. Frequencies of the summed-and-differential harmonic oscillation of the type $[p_2-p_3-p_4]$

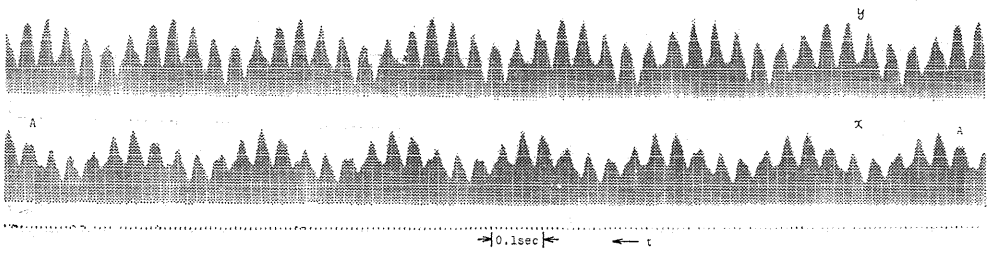

ω=3297 rpm, $\omega : \omega_2 : \omega_3 : \omega_4$=100 : 43 : (−7) : (−50)

Fig. 2. 16. Waves of the summed-and-differential harmonic oscillation of the type $[p_2-p_3-p_4]$

wave with the frequency ω_4 is also present and oscillates 50 times in a backward precession. Since the shaft rotates 100 times in this interval, the relationship $43-(-7)-(-50)=100$, that is, $\omega=\omega_2-\omega_3-\omega_4$ holds.

It is known from Figs. 2.5 and 2.10 that the ranges where the oscillations of the types $[p_2-2p_3]$, $[p_2-2p_4]$, and $[p_2-p_3-p_4]$ due to anisotropic symmetrical nonlinear characteristics occur are fairly narrow when compared with the ranges of the oscillations of the types $[2p_2-p_3]$ and $[2p_2-p_4]$ due to isotropic symmetrical nonlinear characteristics.

The subharmonic oscillation of order 1/3 of forward precession in the neighborhood of $\omega_{\frac{1}{3}}$ where $\omega=3p_2$ holds has a resonance curve of a hard spring type like that of a rectilinear system, as shown in Fig. 2.10. It occurs in the comparatively wide range of $\omega>4120$ rpm. Its vibratory waves are shown in Fig. 2.17. The small wave in this figure is the harmonic component of frequency ω as mentioned previously.

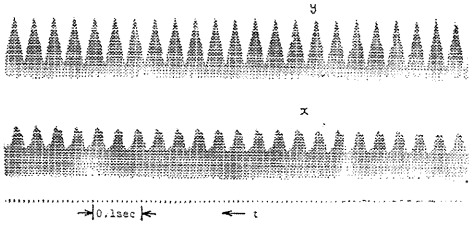

$\omega=4330$rpm, $\omega:\omega_2=3:1$

Fig. 2. 17. Waves of the subharmonic oscillation of the type $[3p_2]$

The oscillations of the types $[2p_2-p_3]$ and $[2p_2-p_4]$ in Fig. 2.5, occurring in the system with isotropic symmetrical nonlinear characteristics, are also found to appear in the system with anisotropic symmetrical nonlinear characteristics. Their general features in the latter system are almost the same as those in the former.

Through many experiments performed in a wide range of ω, no other oscillation due to symmetrical nonlinear characteristics than those mentioned in (Ⅱ-b) occurred.

The experimental results about the occurrence of the oscillations of Eqs. (2.9) and (2.10) in the previous section are shown in Table 2.1. Considerations about Table 2.1 are given in the next chapter.

Table 2. 1. Experimental results about the occurrence of various nonlinear forced oscillations caused by symmetrical nonlinear spring characteristics

Kinds of oscillations / Spring characteristics	Subharmonic oscillations of order 1/3			Summed-and-differential harmonic oscillations						
				Two oscillations						Three oscillations
	$3p_2$	$-3p_3$	$-3p_4$	$2p_2-p_3$	$2p_2-p_4$	p_2-2p_3	p_2-2p_4	$-2p_3-p_4$	$-p_3-2p_4$	$p_2-p_3-p_4$
B-Ⅰ	×	×	×	○	○	×	×	×	×	×
B-Ⅱ	○	×	×	○	○	○	○	×	×	○

B-Ⅰ : Isotropic symmetrical nonlinear spring characteristics (Fig. 4)
B-Ⅱ : Anisotropic symmetrical nonlinear spring characteristics (Fig. 5)
○ …… appearance, × …… non-appearance

(*III*) *Forced oscillations of whirling motion which are influenced by unsymmetrical nonlinear characteristics*

(*III-a*) *Oscillations whose occurrence is influenced*

Various features of these oscillations for the spring characteristics of Fig. 2.3 are the same as those for Fig. 2.4. In other words, the existence of anisotropy of symmetrical nonlinear characteristics does not affect them.

Resonance curves of the subharmonic oscillation of order 1/2 of the type $[2p_2]$ and of summed-and-differential harmonic oscillations of the types $[p_2-p_3]$, $[p_2-p_4]$ are shown in Fig. 2.18. Because of strong symmetrical nonlinear characteristics, their resonance curves become a hard spring type and are bent strongly. The subharmonic oscillation appears in the wide range of $\omega \simeq 2480 \sim 2900$ rpm. The oscillations $[p_2-p_3]$ and $[p_2-p_4]$ appear also in the wide range of $\omega \simeq 1500 \sim 1650$ rpm and $\omega \simeq 2950 \sim 3290$ rpm, respectively.

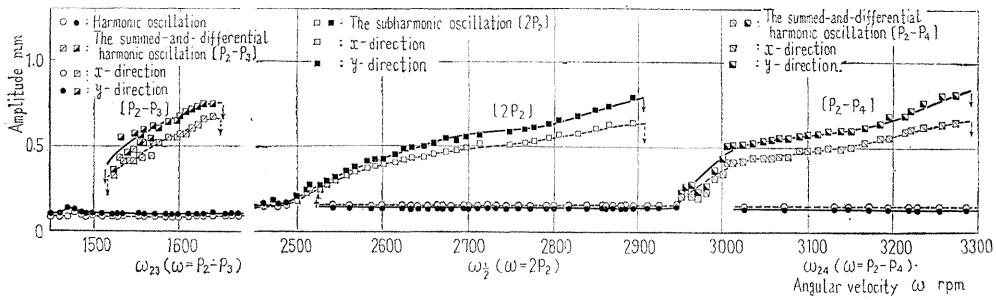

Fig. 2. 18. Oscillations due to unsymmetrical nonlinear spring characteristics

The experimental apparatus of the previous papers[2],[4],[5] are similar to that of Fig. 1.10. Accordingly, by comparing the results of these previous papers with those in Fig. 2.18, we can ascertain the effects of the magnitudes of unsymmetrical and symmetrical nonlinear characteristics to various oscillations caused by unsymmetrical nonlinear characteristics. The experimental results concerning the appearance of the oscillations of Eqs. (2.11) and (2.12) which are expected to occur are summarized in Table 2.2. From this, we can obtain the following conclusions: The oscillations with large amplitudes in the previous papers also appear in this experiment. Those with small amplitudes in the previous papers, however, can not occur in this experiment because of small unsymmetrical nonlinear characteristics. The resonance curves of the oscillations in this experiment are bent strongly toward the higher frequency regions and hence they appears in the wide ranges, because of stronger symmetrical nonlinear characteristics than those in the previous papers.

Table 2. 2. Experimental results about the occurrence of various forced oscillations caused by unsymmetrical nonlinear spring characteristics

Spring characteristics \ Kinds of oscillations		Subharmonic oscillations of order 1/3			Summed-and-differential harmonic oscillations		
		$2p_2$	$-2p_3$	$-2p_4$	p_2-p_3	p_2-p_4	$-p_3-p_4$
A	Appearance or non-appearance	○	△	△	○	○	△
	Width of the range of occurrence (rpm)	25, 40, 150	20, 30	75	100	50, 100, 200	50, 100
	Amplitude	large	small	small	large	large	small
B-Ⅰ	Appearance or non-appearance	○	×	×	○	○	×
B-Ⅱ	Width of the range of occurrence (rpm)	420			150, 200	340	

A …… The case of the previous reports (1), (2), (3), having strong unsymmetrical nonlinear spring characteristics

B-Ⅰ …… The case of Fig. 4 having strong symmetrical nonlinear spring characteristics (isotropic)

B-Ⅱ …… The case of Fig. 5 having strong symmetrical nonlinear spring characteristics (anisotropic)

○……appearance, ×……non-appearance, △……non-appearance or appearance with small amplitude depending on assembly

2. 4. Conclusions

(1) When a shaft is supported by single-row deep groove ball bearing, nonlinear spring characteristics appear in a rotating shaft system. Whether unsymmetrical or symmetrical nonlinear characteristics appear depends on the degree of shift of the shaft center line from the center of an "angular clearance" of a ball bearing.

(2) Being different from the case of a rectilinear system, nonlinear spring characteristics should be considered as two-dimensional distribution in a rotating shaft system.

(3) Symmetrical nonlinear spring characteristics represented by the third powers of coordinates can be classified into the isotropic component and the anisotropic components which change their magnitudes 2 and 4 times while the shaft whirls once.

(4) In the system having only the isotropic symmetrical nolninear characteristics, the summed-and-differential harmonic oscillations of the types $[2p_2-p_3]$ and $[2p_2-p_4]$ occur.

(5) In the system having both the isotropic and anisotropic components of symmetrical nonlinear characteristics, the subharmonic oscillation of order 1/3 of the type $[3p_2]$ and the summed-and-differential harmonic oscillations of the types $[p_2-2p_3]$, $[p_2-2p_4]$, $[p_2-p_3-p_4]$ can occur as well as the types $[2p_2-p_3]$, $[2p_2-p_4]$.

(6) The subharmonic oscillations of order $-1/3$ of the types $[-3p_3]$, $[-3p_4]$ and the summed-and-differential harmonic oscillations of the types $[-2p_3-p_4]$, $[-p_3-2p_4]$ do not occur in the experiments performed in this paper.

(7) In the experiments of the above conclusions (4) and (5), jump phenomena

and hysteresis phenomena, which are induced by the symmetrical nonlinear characteristics, take place in the neighborhoods of the major critical speed and the critical speeds of synchronous backward precession.

(8) Among oscillations due to unsymmetrical nonlinear characteristics, the subharmonic oscillation of order 1/2 of the type $[2p_2]$ and the summed-and-differential harmonic oscillations of the types $[p_2-p_3]$, $[p_2-p_4]$ occur in the experiments in this chapter. The resonance curves of these oscillations bend severely to the higher speed side because of the strong symmetrical nonlinear spring characteristics.

(9) By utilizing the polar coordinate representation of nonlinear spring characteristics, it can be made clear what kinds of nonlinear forced oscillations will occur.

Chapter III. Theoretical Discussions on Vibrations of a Rotating Shaft with Nonlinear Spring Characteristics*

3. 1. Introduction

When the gyroscopic moment acts on a rotating shaft system, lateral vibrations of the shaft are not rectilinear vibrations but whirling motions in the plane perpendicular to the center line of the shaft and passing through the equilibrium position of the rotor[16].

Nonlinear spring characteristics of the shaft are usually expressed by the rectangular coordinate system (x, y). But it is pointed out in this chapter that, for the analytical treatment of nonlinear forced oscillations with modes of whirl, it is advantageous to utilize the polar coordinate system. It is also seen from this chapter that the adoption of polar coordinates helps clarify the properties of nonlinear forced oscillations and it allows the prediction of the occurrence of oscillations to be made. Furthermore, the experimental results of Chapter Ⅱ and of the previous paper[2][4][5] are clearly explained by the theoretical conclusions of this chapter.

Since few oscillations are caused by nonlinear terms of higher than the third power, only unsymmetrical and symmetrical nonlinear characteristics represented by the second and third powers, respectively, are considered here.

3. 2. Spring characteristics and equations of motion

Initially, a system with two degrees of freedom where whirling motions take place is treated. When the rotor is positioned at the middle point of the shaft, deflections and inclinations of the rotor do not couple each other. Accordingly, inclination motions of the rotor can be expressed using only the two coordinates θ_x and θ_y, the components of the inclination angle θ of the rotor in the x- and y-directions. The potential energy V of the system is given by

$$V=1/2\cdot\delta(\theta_x^2+\theta_y^2)+(\varepsilon_{30}\theta_x^3+\varepsilon_{21}\theta_x^2\theta_y+\varepsilon_{12}\theta_x\theta_y^2+\varepsilon_{03}\theta_y^3)$$
$$+(\beta_{40}\theta_x^4+\beta_{31}\theta_x^3\theta_y+\beta_{22}\theta_x^2\theta_y^2+\beta_{13}\theta_x\theta_y^3+\beta_{04}\theta_y^4) \qquad (3.1)$$

where δ is the spring constant, $\varepsilon_{ab}(a+b=3)$ and $\beta_{ab}(a+b=4)$ the small coefficients of the unsymmetrical and symmetrical nonlinear terms, respectively. Adopting the polar coordinates (θ, φ), i. e., substituting

$$\theta_x=\theta\cdot\cos\varphi,\quad \theta_y=\theta\cdot\sin\varphi \tag{3.2}$$

into Eq. (3. 1), we have

$$V=1/2\cdot\delta\theta^2+(\varepsilon_c^{(1)}\cos\varphi+\varepsilon_s^{(1)}\sin\varphi+\varepsilon_c^{(3)}\cos 3\varphi+\varepsilon_s^{(3)}\sin 3\varphi)\theta^3$$
$$+(\beta^{(0)}+\beta_c^{(2)}\cos 2\varphi+\beta_s^{(2)}\sin 2\varphi+\beta_c^{(4)}\cos 4\varphi+\beta_s^{(4)}\sin 4\varphi)\theta^4 \tag{3.3}$$

The number of the coefficients in Eq. (3. 3) is the same as that in Eq. (3. 1) and the next relationships hold between them.

$$\left.\begin{aligned}
&\varepsilon_c^{(1)}=(3\varepsilon_{30}+\varepsilon_{12})/4, && \varepsilon_s^{(1)}=(\varepsilon_{21}+3\varepsilon_{03})/4,\\
&\varepsilon_c^{(3)}=(\varepsilon_{30}-\varepsilon_{12})/4, && \varepsilon_s^{(3)}=(\varepsilon_{21}-\varepsilon_{03})/4,\\
&\beta^{(0)}=(3\beta_{40}+\beta_{22}+3\beta_{04})/8, &&\\
&\beta_c^{(2)}=(\beta_{40}-\beta_{04})/2, && \beta_s^{(2)}=(\beta_{31}+\beta_{13})/4,\\
&\beta_c^{(4)}=(\beta_{40}-\beta_{22}+\beta_{04})/8, && \beta_s^{(4)}=(\beta_{31}-\beta_{13})/8,
\end{aligned}\right\} \tag{3.4}$$

Equation (3. 3) is transformed into

$$V=1/2\cdot\delta\theta^2+\{\varepsilon^{(1)}\cos(\varphi-\varphi_1)+\varepsilon^{(3)}\cos 3(\varphi-\varphi_3)\}\theta^3$$
$$+\{\beta^{(0)}+\beta^{(2)}\cos 2(\varphi-\varphi_2)+\beta^{(4)}\cos 4(\varphi-\varphi_4)\}\theta^4 \tag{3.3a}$$

where

$$\left.\begin{aligned}
&\varepsilon^{(1)}=\sqrt{\varepsilon_c^{(1)2}+\varepsilon_s^{(1)2}}, && \varepsilon^{(3)}=\sqrt{\varepsilon_c^{(3)2}+\varepsilon_s^{(3)2}},\\
&\beta^{(2)}=\sqrt{\beta_c^{(2)2}+\beta_s^{(2)2}}, && \beta^{(4)}=\sqrt{\beta_c^{(4)2}+\beta_s^{(4)2}},\\
&\varphi_1=\tan^{-1}(\varepsilon_s^{(1)}/\varepsilon_c^{(1)}), && \varphi_3=1/3\cdot\tan^{-1}(\varepsilon_s^{(3)}/\varepsilon_c^{(3)}),\\
&\varphi_2=1/2\cdot\tan^{-1}(\beta_s^{(2)}/\beta_c^{(2)}), && \varphi_4=1/4\cdot\tan^{-1}(\beta_s^{(4)}/\beta_c^{(4)}).
\end{aligned}\right\} \tag{3.5}$$

The potential energy V is illustrated in Fig. 3. 1, in which the paraboloid shown by the broken line curves is $V=V_0=1/2\cdot\delta\ (\theta_x^2+\theta_y^2)$ of the linear system. The potential energy of Eqs. (3. 1), (3. 3), and (3. 3a), shown by solid line curves deviates irregularly from V_0, because of the nonlinear characteristics. But by adopting polar coordinates, these characteristics can be classified into regular components as shown in Figs. 3. 2 and 3. 3. Figures 3. 2 and 3. 3 show the cross section of the curved surface V with a plane parallel to the $\theta_x\theta_y$-plane, in cases that $\varepsilon^{(1)}$, $\varepsilon^{(3)}$ and $\beta^{(0)}$, $\beta^{(2)}$, $\beta^{(4)}$, exist, respectively. It is seen that $\varepsilon_s^{(n)}$, $\beta_c^{(n)}$, etc. are coefficients of terms varying their magnitude n times while the angle φ changes its value from 0 to 2π. In this paper, these components of nonlinear characteristics are denoted by the notation N(n)). Only Fig. 3. 3(i) is the case which has no anisotropy.

Next we consider a system with four degrees of freedom in which the deflection r and the inclination of the rotor couple each other. Let the mass of the rotor be m, the polor and diametral moments of inertia of the rotor be I_p and I, respectively, the deflections and inclination angles of the rotor be x, y and θ_x, θ_y, the spring

constants of the shaft be α, γ, and δ, the static and dynamic unbalances of the rotor be e and τ, the angle between e and τ be β, and the damping coefficients be c_{ab}. Introducing the dimensionless quantities :

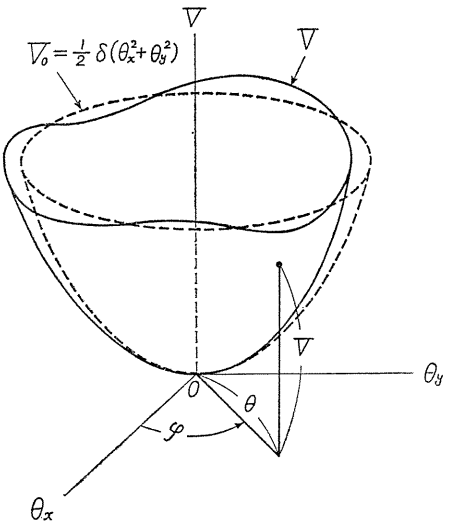

Fig. 3. 1. The distribution of potential energy V

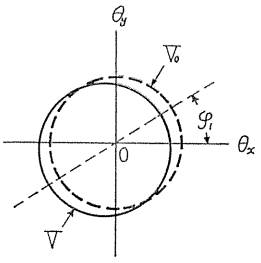

(i) $V=V_0+\varepsilon^{(1)}\cos(\varphi-\varphi_1)\cdot\theta^3$

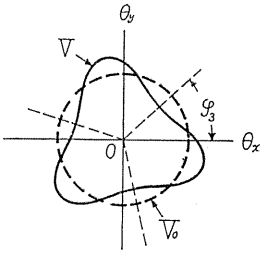

(ii) $V=V_0+\varepsilon^{(3)}\cos 3(\varphi-\varphi_3)\cdot\theta^3$

Fig. 3. 2. Unsymmetrical Nonlinear Spring Characteristics

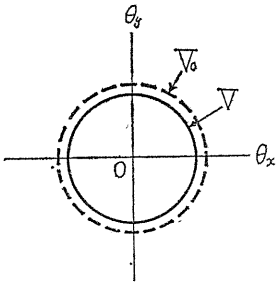

(i) $V=V_0+\beta^{(0)}\theta^4$

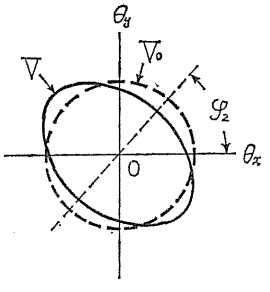

(ii) $V=V_0+\beta^{(2)}\cos 2(\varphi-\varphi_2)\theta^4$

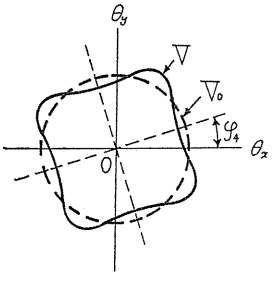

(iii) $V=V_0+\beta^{(4)}\cos 4(\varphi-\varphi_4)\theta^4$

Fig. 3. 3. Symmetrical Nonlinear Spring Characteristics

$$\left.\begin{aligned} &x'=x/\sqrt{I/m}, && y'=y/\sqrt{I/m}, && e'=e/\sqrt{I/m},\\ &c'_{11}=c_{11}/\sqrt{\alpha m}, && c'_{12}=c_{12}/\sqrt{\alpha I}=c'_{21}=c_{21}/\sqrt{\alpha I}, &&\\ &c'_{22}=c_{22}/(I\sqrt{\alpha/m}), && \omega'=\omega/\sqrt{\alpha/m}, && t'=t\sqrt{\alpha/m},\\ &\gamma'=\gamma/(\alpha\sqrt{I/m}), && \delta'=\delta m/(\alpha I), && i_p=I_p/I, \end{aligned}\right\} \quad (3.6)$$

and omitting the prime, we have the following equations of motion represented by dimensionless quantities

$$\left.\begin{aligned} &\ddot{x}+c_{11}\dot{x}+c_{12}\dot{\theta}_x+x+\gamma\theta_x+\psi_x+\varphi_x=e\omega^2\cos\omega t\\ &\ddot{y}+c_{11}\dot{y}+c_{12}\dot{\theta}_y+y+\gamma\theta_y+\psi_y+\varphi_y=e\omega^2\sin\omega t\\ &\ddot{\theta}_x+i_p\omega\dot{\theta}_y+c_{21}\dot{x}+c_{22}\dot{\theta}_x+\gamma x+\delta\theta_x+\psi_{\theta x}+\varphi_{\theta x}=(i_p-1)\tau\omega^2\cos(\omega t+\beta)\\ &\ddot{\theta}_y-i_p\omega\dot{\theta}_x+c_{21}\dot{y}+c_{22}\dot{\theta}_y+\gamma y+\delta\theta_y+\psi_{\theta y}+\varphi_{\theta y}=(i_p-1)\tau\omega^2\sin(\omega t+\beta) \end{aligned}\right\} \quad (3.7)$$

in which ψ_x, $\psi_{\theta y}$, etc., and φ_x $\varphi_{\theta y}$, etc., are unsymmetrical and symmetrical, nonlinear terms, respectively. The frequency equation of the system is

$$f(p)=(1-p^2)(\delta+i_p\omega p-p^2)-\gamma^2=0 \quad (3.8)$$

where p is the natural frequency. Between the four natural frequencies $p_{1,2,3,4}$, the following relationships hold:

$$\left.\begin{aligned} &p_1>p_{10}>1>p_2>0>p_3>-1>p_4>-p_{10}, \quad p_1>i_p\omega,\\ &p_{10}^2=\{(1+\delta)+\sqrt{(1+\delta)^2-4(\delta-\gamma^2)}\}/2. \end{aligned}\right\} \quad (3.9)$$

By the linear transformations

$$x=\sum_{s=1}^{4}X_s, \quad y=-\sum_{s=1}^{4}(X_s/p_s), \quad \theta_x=\sum_{s=1}^{4}\kappa_sX_s, \quad \theta_y=-\sum_{s=1}^{4}(\kappa_s\dot{X}_s/p_s) \quad (3.10)$$

the following equations of motion represented by the normal coordinates X_s are given as follows[6]:

$$\begin{aligned} \ddot{X}_s+\omega_s^2X_s=(\omega_s^2-p_s^2)X_s+n_s\Big[&\Big\{\frac{c_{11}(-\dot{x}+p_sy)}{\kappa_s}\\ &+c_{12}\Big(-\dot{x}+p_sy-\frac{\theta_x}{\kappa_s}+\frac{p_s\theta_y}{\kappa_s}\Big)+c_{22}(-\dot{\theta}_x+p_s\theta_y)\Big\}\\ &+\Big\{-\frac{(\psi_x+\varphi_x)}{\kappa_s}-(\psi_{\theta x}+\varphi_{\theta x})+\frac{p_s(\Psi_y+\Phi_y)}{\kappa_s}+p_s(\Psi_{\theta y}+\Phi_{\theta y})\\ &+\omega(\omega+p_s)\Big\{\frac{e}{\kappa_s}\cos\omega t+(i_p-1)\tau\cos(\omega t+\beta)\Big\}\Big] \end{aligned}$$

$$(s=1,\ 2,\ 3,\ 4) \quad (3.11)$$

where

$$\kappa_s=\frac{(p_s^2-1)}{\gamma},\quad n_s=\frac{\gamma p_s}{(p_s-p_i)(p_s-p_j)(p_s-p_k)}$$
$$(s\neq i\neq j\neq k,\ i,\ j,\ k,\ s=1,\ 2,\ 3,\ 4) \tag{3.12}$$

and Ψ_y, Φ_y, Ψ_{0y}, and Φ_{0y} are the infinite integrals of ψ_y, φ_y, ψ_{0y}, and ψ_{0y}, respectively.

Since nonlinear terms are limited to no higher than the third order, the number of nonlinear forced vibrations appearing simultaneously, that is, vibration components but that of frequency ω, must not exceed three. As the solution of Eq. (3. 11), we have

$$X_s=R_s\cos(\omega_s t+\delta_s)+A_s\cos\omega t+B_s\sin\omega t. \tag{3.13}$$

When small quantities are rejected, Eq. (3. 13) leads to

$$\left.\begin{aligned}\begin{matrix}x\\y\end{matrix}&=R_i\begin{matrix}\cos\\\sin\end{matrix}(\omega_i t+\delta_i)+R_j\begin{matrix}\cos\\\sin\end{matrix}(\omega_j t+\delta_j)+R_k\begin{matrix}\cos\\\sin\end{matrix}(\omega_k t+\delta_k)\\&\quad+F_1\begin{matrix}\cos\\\sin\end{matrix}\omega t\mp F_2\begin{matrix}\sin\\\cos\end{matrix}\omega t\\\begin{matrix}\theta_x\\\theta_y\end{matrix}&=\kappa_i R_i\begin{matrix}\cos\\\sin\end{matrix}(\omega_i t+\delta_i)+\kappa_j R_j\begin{matrix}\cos\\\sin\end{matrix}(\omega_j t+\delta_j)+\kappa_k R_k\begin{matrix}\cos\\\sin\end{matrix}(\omega_k t+\delta_k)\\&\quad+F_3\begin{matrix}\cos\\\sin\end{matrix}\omega t\mp F_4\begin{matrix}\sin\\\cos\end{matrix}\omega t\\&\qquad(i,\ j,\ k=1,\ 2,\ 3,\ 4,\quad i\neq j\neq k)\end{aligned}\right\} \tag{3.14}$$

where

$$\left.\begin{aligned}F_1&=\frac{\omega^2[\{\delta+(i_p-1)\omega^2\}e-\gamma(i_p-1)\tau\cos\beta]}{f(\omega)}\\F_2&=-\frac{\gamma(i_p-1)\tau\omega^2\sin\beta}{f(\omega)}\\F_3&=\frac{\omega^2\{-e\gamma+(1-\omega^2)(i_p-1)\tau\cos\beta\}}{f(\omega)}\\F_4&=\frac{(1-\omega^2)(i_p-1)\tau\omega^2\sin\beta}{f(\omega)}\end{aligned}\right\} \tag{3.15}$$

and $f(\omega)$ means $[f(p)]_{p=\omega}$ in Eq. (3. 8).

The potential energy for this system is expressed by

$$V=\{\frac{1}{2}(x^2+y^2)+\gamma(x\theta_x+y\theta_y)+\frac{1}{2}\delta(\theta_x^2+\theta_y^2)+\sum_{\substack{a,\ b,\ c,\ d=0\\(a+b+c+d=3)}}^{3}\varepsilon_{abcd}x^a y^b\theta_x^c\theta_y^d$$
$$+\sum_{\substack{a,\ b,\ c,\ d=0\\(a+b+c+d=4)}}^{4}\beta_{abcd}x^a y^b\theta_x^c\theta_y^d \tag{3.16}$$

Restoring forces are given by

$$F_x=-\frac{\partial V}{\partial x},\quad F_y=-\frac{\partial V}{\partial y},\quad F_{\theta x}=-\frac{\partial V}{\partial \theta_x},\quad F_{\theta y}=-\frac{\partial V}{\partial \theta_y}. \tag{3.17}$$

By inserting

$$x=r\cos\varphi_r,\quad y=r\sin\varphi_r,\quad \theta_x=\theta\cos\varphi_\theta,\quad \theta_y=\theta\sin\varphi_\theta \tag{3.18}$$

into Eq. (3. 16), we get the potential energy V in polar coordinates.

$$\begin{aligned}
V=&\{\frac{1}{2}r^2+\gamma r\theta\cos(\varphi_r-\varphi_\theta)+\frac{1}{2}\delta\theta^2\}\\
&+\Big[[(\varepsilon^{(1)}_{30c}\cos\varphi_r+\varepsilon^{(1)}_{30s}\sin\varphi_r)r^3+\{\varepsilon^{(1)}_{21c}\cos\varphi_\theta+\varepsilon^{(1)}_{21s}\sin\varphi_\theta\\
&+\varepsilon'^{(1)}_{21c}\cos(2\varphi_r-\varphi_\theta)+\varepsilon'^{(1)}_{21s}\sin(2\varphi_r-\varphi_\theta)\}r^2\theta+\{\varepsilon^{(1)}_{12c}\cos\varphi_r+\varepsilon^{(1)}_{12s}\sin\varphi_r\\
&+\varepsilon'^{(1)}_{12c}\cos(2\varphi_\theta-\varphi_r)+\varepsilon'^{(1)}_{12s}\sin(2\varphi_\theta-\varphi_r)\}r\theta^2+(\varepsilon^{(1)}_{03c}\cos\varphi_\theta+\varepsilon^{(1)}_{03s}\sin\varphi_\theta)\theta^3]\\
&+(\varepsilon^{(3)}_{30c}\cos 3\varphi_r+\varepsilon^{(3)}_{30s}\sin 3\varphi_r)r^3+\{\varepsilon^{(3)}_{21c}\cos(2\varphi_r+\varphi_\theta)+\varepsilon^{(3)}_{21s}\sin((2\varphi_r+\varphi_\theta)\}r^2\theta\\
&+\{\varepsilon^{(3)}_{12c}\cos(2\varphi_\theta+\varphi_r)+\varepsilon^{(3)}_{12s}\sin(2\varphi_\theta+\varphi_r)\}r\theta^2+(\varepsilon^{(3)}_{03c}\cos 3\varphi_\theta+\varepsilon^{(3)}_{03s}\sin 3\varphi_\theta)\theta^3]\Big]\\
&+\Big[[\beta^{(0)}_{40}r^4+\{\beta^{(0)}_{31c}\cos(\varphi_r-\varphi_\theta)+\beta^{(0)}_{31s}\sin(\varphi_r-\varphi_\theta)\}r^3\theta+\{\beta^{(0)}_{22}+\beta^{(0)}_{22c}\cos 2(\varphi_r-\varphi_\theta)\\
&+\beta^{(0)}_{22s}\sin 2(\varphi_r-\varphi_\theta)\}r^2\theta^2+\{\beta^{(0)}_{13c}\cos(\varphi_\theta-\varphi_r)+\beta^{(0)}_{13s}\sin(\varphi_\theta-\varphi_r)\}r\theta^3+\beta^{(0)}_{04}\theta^4]\\
&+[(\beta^{(2)}_{40c}\cos 2\varphi_r+\beta^{(2)}_{40s}\sin 2\varphi_r)r^4+\{\beta^{(2)}_{31c}\cos(\varphi_r+\varphi_\theta)+\beta^{(2)}_{31s}\sin(\varphi_r+\varphi_\theta)\\
&+\beta'^{(2)}_{31c}\cos(3\varphi_r-\varphi_\theta)+\beta'^{(2)}_{31s}\sin(3\varphi_r-\varphi_\theta)\}r^3\theta+\{\beta^{(2)}_{22c}\cos 2\varphi_r+\beta^{(2)}_{22s}\sin 2\varphi_r\\
&+\beta'^{(2)}_{22c}\cos 2\varphi_\theta+\beta'^{(2)}_{22s}\sin 2\varphi_\theta\}r^2\theta^2+\{\beta^{(2)}_{13c}\cos(\varphi_\theta+\varphi_r)+\theta^{(2)}_{13s}\sin(\varphi_\theta+\varphi_r)\\
&+\beta'^{(2)}_{13c}\cos(3\varphi_\theta-\varphi_r)+\beta'^{(2)}_{13s}\sin(3\varphi_\theta-\varphi_r)\}r\theta^3+(\beta^{(2)}_{04c}\cos 2\varphi_\theta+\beta^{(2)}_{04s}\sin 2\varphi_\theta)\theta^4]\\
&+[(\beta^{(4)}_{40c}\cos 4\varphi_r+\beta^{(4)}_{40s}\sin 4\varphi_r)r^4+\{\beta^{(4)}_{31c}\cos(3\varphi_r+\varphi_\theta)+\beta^{(4)}_{31s}\sin(3\varphi_r+\varphi_\theta)\}r^3\theta\\
&+\{\beta^{(4)}_{22c}\cos 2(\varphi_r+\varphi_\theta)+\beta^{(4)}_{22s}\sin 2(\varphi_r+\varphi_\theta)\}r^2\theta^2+\{\beta^{(4)}_{13c}\cos(3\varphi_\theta+\varphi_r)\\
&+\beta^{(4)}_{13s}\sin(3\varphi_\theta+\varphi_r)\}r\theta^3+(\beta^{(4)}_{04c}\cos 4\varphi_\theta+\beta^{(4)}_{04s}\sin 4\varphi_\theta)\}\theta^4]\Big]
\end{aligned} \tag{3.19}$$

in which, for instance, the angle $\varphi_r-\varphi_\theta$ is constant and terms containing $\varphi_r-\varphi_\theta$, $2\varphi_r-\varphi_\theta$, $3\varphi_r-\varphi_\theta$, $2\varphi_r+\varphi_\theta$, and $3\varphi_r+\varphi_\theta$ are components expressed by N(0), N(1), N(2), N(3), and N(4), respectively. There exist the following relationships:

$$\varepsilon^{(1)}_{30c}=(3\varepsilon_{3000}+\varepsilon_{1200})/4,\qquad \varepsilon^{(1)}_{30s}=(3\varepsilon_{0300}+\varepsilon_{2100})/4,$$

$$\varepsilon^{(1)}_{21c}=(\varepsilon_{2010}+\varepsilon_{0210})/2,\qquad \varepsilon^{(1)}_{21s}=(\varepsilon_{0201}+\varepsilon_{2001})/2,$$

$$\varepsilon'^{(1)}_{21c}=(\varepsilon_{2010}+\varepsilon_{1101}-\varepsilon_{0210})/4, \qquad \varepsilon'^{(1)}_{21s}=(\varepsilon_{0201}+\varepsilon_{1110}-\varepsilon_{2001})/4,$$

$$\varepsilon^{(1)}_{12c}=(\varepsilon_{1020}+\varepsilon_{1002})/2, \qquad \varepsilon^{(1)}_{12s}=(\varepsilon_{0102}+\varepsilon_{0120})/2,$$

$$\varepsilon'^{(1)}_{12c}=(\varepsilon_{1020}+\varepsilon_{0111}-\varepsilon_{1002})/4, \qquad \varepsilon'^{(1)}_{12s}=(\varepsilon_{0102}+\varepsilon_{1011}-\varepsilon_{0120})/4,$$

$$\varepsilon^{(1)}_{03c}=(3\varepsilon_{0030}+\varepsilon_{0012})/4, \qquad \varepsilon^{(1)}_{03s}=(3\varepsilon_{0003}+\varepsilon_{0021})/4,$$

$$\varepsilon^{(3)}_{30c}=(\varepsilon_{3000}-\varepsilon_{1200})/4, \qquad \varepsilon^{(3)}_{30s}=(-\varepsilon_{0300}+\varepsilon_{2100})/4,$$

$$\varepsilon^{(3)}_{21c}=(\varepsilon_{2010}-\varepsilon_{1101}-\varepsilon_{0210})/4, \qquad \varepsilon^{(3)}_{21s}=(-\varepsilon_{0201}+\varepsilon_{1110}+\varepsilon_{2001})/4,$$

$$\varepsilon^{(3)}_{12c}=(\varepsilon_{1020}-\varepsilon_{0111}-\varepsilon_{1002})/4, \qquad \varepsilon^{(3)}_{12s}=(-\varepsilon_{0102}+\varepsilon_{1011}+\varepsilon_{0120})/4,$$

$$\varepsilon^{(3)}_{03c}=(\varepsilon_{0030}-\varepsilon_{0012})/4, \qquad \varepsilon^{(3)}_{03s}=(-\varepsilon_{0003}+\varepsilon_{0021})/4,$$

$$\beta^{(0)}_{40}=\{3(\beta_{4000}+\beta_{0400})+\beta_{2200}\}/8, \qquad \beta^{(0)}_{04}=\{3(\beta_{0040}+\beta_{0004})+\beta_{0022}\}/8,$$

$$\beta^{(0)}_{22}=(\beta_{2020}+\beta_{0202}+\beta_{2002}+\beta_{0220})/4,$$

$$\beta^{(0)}_{31c}=\{3(\beta_{3010}+\beta_{0301})+(\beta_{2101}+\beta_{1210})\}/8,$$

$$\beta^{(0)}_{31s}=\{-3(\beta_{3001}-\beta_{0310})+(\beta_{2110}-\beta_{1201})\}/8,$$

$$\beta^{(0)}_{22c}=(\beta_{2020}+\beta_{0202}-\beta_{2002}-\beta_{0220}+\beta_{1111})/8, \quad \beta^{(0)}_{22s}=(\beta_{0211}+\beta_{1120}-\beta_{2011}-\beta_{1102})/8,$$

$$\beta^{(0)}_{13c}=\{3(\beta_{1030}+\beta_{0103})+(\beta_{0121}+\beta_{1012})\}/8,$$

$$\beta^{(0)}_{13s}=\{3(\beta_{1003}-\beta_{0130})+(\beta_{1021}-\beta_{0112})\}/8,$$

$$\beta^{(2)}_{40c}=(\beta_{4000}-\beta_{0400})/2, \qquad \beta^{(2)}_{40s}=(\beta_{3100}+\beta_{1300})/4,$$

$$\beta^{(2)}_{31c}=\{3(\beta_{3010}-\beta_{0301})-(\beta_{2101}-\beta_{1210})\}/8,$$

$$\beta^{(2)}_{31s}=\{3(\beta_{3001}+\beta_{0310})+(\beta_{2110}+\beta_{1201})\}/8,$$

$$\beta'^{(2)}_{31c}=(\beta_{3010}-\beta_{0301}+\beta_{2101}-\beta_{1210})/8, \qquad \beta'^{(2)}_{31s}=(-\beta_{3001}-\beta_{0310}+\beta_{2110}+\beta_{1201})/8,$$

$$\beta^{(2)}_{22c}=(\beta_{2020}-\beta_{0202}+\beta_{2002}-\beta_{0220})/4, \qquad \beta^{(2)}_{22s}=(\beta_{1120}+\beta_{1102})/4,$$

$$\beta'^{(2)}_{22c}=(\beta_{2020}-\beta_{0202}-\beta_{2002}+\beta_{0220})/4, \qquad \beta'^{(2)}_{22s}=(\beta_{2011}+\beta_{0211})/4,$$

$$\beta^{(2)}_{13c}=\{3(\beta_{1030}-\beta_{0103})-(\beta_{0121}-\beta_{1012})\}/8,$$

$$\beta^{(2)}_{13s}=\{3(\beta_{0130}+\beta_{1003})+(\beta_{1021}+\beta_{0112})\}/8,$$

$$\beta'^{(2)}_{13c}=(\beta_{1030}-\beta_{0103}+\beta_{0121}-\beta_{1012})/8, \qquad \beta'^{(2)}_{13s}=(-\beta_{0130}-\beta_{1003}+\beta_{1021}+\beta_{0112})/8,$$

$$\beta^{(2)}_{04c}=(\beta_{0040}-\beta_{0004})/2, \qquad \beta^{(2)}_{04s}=(\beta_{0031}+\beta_{0013})/4,$$

$$\beta^{(4)}_{40c}=(\beta_{4000}+\beta_{0400}-\beta_{2200})/8, \qquad \beta^{(4)}_{40s}=(\beta_{3100}-\beta_{1300})/8,$$

$$\beta^{(4)}_{31c}=(\beta_{3010}+\beta_{0301}-\beta_{2101}-\beta_{1210})/8, \qquad \beta^{(4)}_{31s}=(\beta_{3001}-\beta_{0310}+\beta_{2110}-\beta_{1201})/8,$$

$$\beta^{(4)}_{22c}=(\beta_{2020}+\beta_{0202}-\beta_{2002}-\beta_{0220}-\beta_{1111})/8,\quad \beta^{(4)}_{22s}=(\beta_{2011}+\beta_{1120}-\beta_{1102}-\beta_{0211})/8,$$

$$\beta^{(4)}_{13c}=(\beta_{1030}+\beta_{0103}-\beta_{0121}-\beta_{1012})/8,\qquad \beta^{(4)}_{13s}=(\beta_{0130}-\beta_{1003}+\beta_{1021}-\beta_{0112})/8,$$

$$\beta^{(4)}_{04c}=(\beta_{0040}+\beta_{0004}-\beta_{0022})/8,\qquad \beta^{(4)}_{04s}=(\beta_{0031}-\beta_{0013})/8. \tag{3.20}$$

where $\beta^{(n)}_{abc}$ and $\varepsilon^{(n)}_{absc}$ represent coefficients of the nonlinear component N(n).

3. 3. A classification of nonlinear forced oscillations

It is proved that, among summed-and-differential harmonic oscillations, only vibrations with modes of the summed type with respect to the absolute values of frequencies can take place[10]. Accordingly, only the vibrations in Table 3. 1 can be expected to occur, because $p_1>0$, $p_2>0$, $p_3<0$, $p_4<0$ hold.

3. 4. Various nonlinear forced oscillations

Substituting Eqs. (3. 13) and (3. 14) into the right-hand side of Eq. (3. 11), we get the terms of frequency ω with the following form:

$$(C_s-C'_s)\cos(\omega_s t+\delta_s)+(S_s-S'_s)\sin(\omega_s t+\delta_s)$$

Since resonance terms should vanish, we have

$$C_s=C'_s,\quad S_s=S'_s\quad (s=i,\ j,\ k,\ i\neq j\neq k,\ i,\ j,\ k=1,\ 2,\ 3,\ 4). \tag{3.21}$$

From Eq. (3. 21), equations for resonance curves, backbone curves, frequencies, and phase angles are derived. In Eq. (3. 21), C_s, and S_s are coefficients which are obtainable independent of the kind of oscillations, i. e. of the relationships in Table 3. 1. After some calculations, C_s and S_s are given as follows:

$$\left.\begin{aligned} C_s&=[(\omega_s^2-p_s^2)-n_s\{2(\rho^{(0)}_{si}R_i^2+\rho^{(0)}_{sj}R_j^2+\rho^{(0)}_{sk}R_k^2)-\rho^{(0)}_{ss}R_s^2+(\beta^{(0)}F^2)_s\}]R_s\\ S_s&=2n_sc_s\omega_sR_s\\ &\qquad (s=i,\ j,\ k,\ i\neq j\neq k,\ i,\ j,\ k=1,\ 2,\ 3,\ 4)\end{aligned}\right\} \tag{3.22}$$

$$\left.\begin{aligned} \rho^{(0)}_{si}&=2\{4\beta^{(0)}_{40}+2(\kappa_i+\kappa_s)\beta^{(0)}_{31c}+(\kappa_i+\kappa_s)^2\beta^{(0)}_{22}+4\kappa_i\kappa_s\beta^{(0)}_{22c}\\ &\quad+2\kappa_i\kappa_s(\kappa_i+\kappa_s)\beta^{(0)}_{13c}+4\kappa_i^2\kappa_s^2\beta^{(0)}_{04}\}/\kappa_s\\ (\beta^{(0)}F^2)_s&=4(4\beta^{(0)}_{40}/\kappa_s+2\beta^{(0)}_{31c}+\kappa_s\beta^{(0)}_{22})(F_1^2+F_2^2)+8(\beta^{(0)}_{31c}/\kappa_s+\beta^{(0)}_{22}+2\beta^{(0)}_{22c}\\ &\quad+\kappa_s\beta^{(0)}_{13c})(F_1F_3+F_2F_4)+4(\beta^{(0)}_{22}/\kappa_s+2\beta^{(0)}_{13c}+4\kappa_s\beta^{(0)}_{04})(F_3^2+F_4^2)\\ &\quad+8(\beta^{(0)}_{31s}/\kappa_s+2\beta^{(0)}_{22s}-\kappa_s\beta^{(0)}_{13s})(F_2F_3-F_1F_4)\\ c_s&=c_{11}/\kappa_s+2c_{12}+\kappa_sc_{22}\end{aligned}\right\} \tag{3.23}$$

C_s consists of only coefficients β_{abcd}, and these are reduced to coefficients of N(0) by Eq. (3. 20) as shown above.

Since C_s contains only coefficients of N(0), it is determined solely by N(0) whether resonance curves belong to the hard or soft spring type.

In Eq. (3. 21), C'_s and S'_s are derived from the relationships in Table 3. 1. Consequently, C'_s and S'_s vary for the different kinds of oscillations. It is noticed

Table 3. 1. Classification of Various nonlinear forced oscillations and the components required for their occurrences

Systems with four degrees of freedom

			Precessional motion	Kinds of oscillations	Necessary nonlinear components
Forced oscillations caused by symmetrical nonlinear characteristics	Subharmonic oscillations of order 1/3		Forward	$\omega \fallingdotseq 3p_1$ (appear when $i_p<1/3$) $\omega \fallingdotseq 3p_2$	N(0), N(2)
			Backward	$\omega \fallingdotseq -3p_3$ $\omega \fallingdotseq -3p_4$	N(0), N(4)
	Summed-and-differential harmonic oscillations	Two oscillations	Forward + Forward	$\omega \fallingdotseq 2p_1+p_2$ ($i_p<1/2$) $\omega \fallingdotseq p_1+2p_2$ ($i_p<1$)	N(0), N(2)
			Forward + Backward (2 × forward)	$\omega \fallingdotseq 2p_1-p_3$ ($i_p<1/2$), $\omega \fallingdotseq 2p_2-p_3$* $\omega \fallingdotseq 2p_1-p_4$ ($i_p<1/2$), $\omega \fallingdotseq 2p_2-p_4$	N(0)
			Forward + Backward (2 × backward)	$\omega \fallingdotseq p_1-2p_3$ ($i_p<1$), $\omega \fallingdotseq p_2-2p_3$ $\omega \fallingdotseq p_1-2p_4$ ($i_p<1$), $\omega \fallingdotseq p_2-2p_4$	N(0), N(2)
			Backward + Backward	$\omega \fallingdotseq -2p_3-p_4$ $\omega \fallingdotseq -p_3-2p_4$	N(0), N(4)
		Three oscillations	Forward + Forward + Backward	$\omega \fallingdotseq p_1+p_2-p_3$ ($i_p<1$) $\omega \fallingdotseq p_1+p_2-p_4$ ($i_p<1$)	N(0)
			Forward + Backward + Backward	$\omega \fallingdotseq p_1-p_3-p_4$ ($i_p<1$) $\omega \fallingdotseq p_2-p_3-p_4$	N(0), N(2)
Forced oscillations caused by unsymmetrical nonlinear characteristics	Subharmonic oscillations of order 1/2		Forward	$\omega \fallingdotseq 2p_1$ ($i_p<1/2$) $\omega \fallingdotseq 2p_2$	N(0), N(1)
			Backward	$\omega \fallingdotseq -2p_3$ $\omega \fallingdotseq -2p_4$	N(0), N(3)
	Summed-and-differential harmonic oscillations		Forward + Forward	$\omega \fallingdotseq p_1+p_2$ ($i_p<1$)	N(0), N(1)
			Forward + Backward	$\omega \fallingdotseq p_1-p_3$ ($i_p<1$), $\omega \fallingdotseq p_2-p_3$ $\omega \fallingdotseq p_1-p_4$ ($i_p<1$), $\omega \fallingdotseq p_2-p_4$	N(0), N(1)
			Backward + Backward	$\omega \fallingdotseq -p_3-p_4$	N(0), N(3)

* This equation means that two oscillations, whose frequencies are ω_2 and ω_3 and the relationships $\omega=2\omega_2-\omega_3$, $\omega_2 \fallingdotseq p_2$, $\omega_3 \fallingdotseq p_3$ hold, appear simultaneously in the neighborhood of the rotating speed $\omega \fallingdotseq 2p_2-p_3$.

that, for each kind of oscillation, C_s' and S_s' consist of only one component from among N(0), N(1), N(2), N(3), and N(4), as will be shown later.

When three oscillations occur simultaneously, C_s is given by Eq. (3.22) directly. Putting $R_k=0$ and $R_j=R_k=0$ in Eq. (3.22), C_s is obtained for the cases in which two and one oscillations occur, respectively. In the following, we show the concrete form of Eq. (3.21) for each nonlinear oscillation.

I. Forced oscillations caused by symmetrical nonlinear spring characteristics

A. Subharmonic oscillations of order 1/3.

(a) Oscillations of $\omega=3\omega_i\fallingdotseq 3p_i$ $(i=1, 2)$

$$\left.\begin{aligned}\frac{1}{n_i}\left(\frac{1}{9}\omega^2-p_i^2\right)-\{\rho^{(0)}_{i\,i}R_i^2+(\beta^{(0)}F^2)_i\}&=\frac{R_i}{\kappa_i}\{(\beta^{(2)}F)_{ii}\cos 3\delta_i+(\beta^{(2)}F)'_{i\,i}\sin 3\delta_i\}\\ \frac{2}{3}c_i\omega&=\frac{R_i}{\kappa_i}\{(\beta^{(2)}F)_{ii}\sin 3\delta_i-(\beta^{(2)}F)'_{i\,i}\cos 3\delta_i\}\end{aligned}\right\}\tag{3.24}$$

(b) Oscillations of $\omega=-3\omega_k\fallingdotseq -3p_k$ $(k=3, 4)$

$$\left.\begin{aligned}\frac{1}{n_k}\left(\frac{1}{9}\omega^2-p_k^2\right)-\{\rho^{(0)}_{k\,k}R_k^2+(\beta^{(0)}F^2)_k\}&=\frac{R_k}{\kappa_k}\{(\beta^{(4)}F)_{kk}\cos 3\delta_k+(\beta^{(4)}F)'_{k\,k}\sin 3\delta_k\}\\ \frac{2}{3}c_k\omega&=\frac{R}{\kappa_k}\{-(\beta^{(4)}F)_{kk}\sin 3\delta_k+(\beta^{(4)}F)'_{k\,k}\cos 3\delta_k\}\end{aligned}\right\}\tag{3.25}$$

B. Summed-and-differential harmonic oscillations consisting of two vibrations

(c) Oscillations of $\omega=2\omega_i+\omega_j\fallingdotseq 2p_i+p_j$ $(i, j=1, 2, i\neq j)$

$$\left.\begin{aligned}&\left[\frac{1}{n_i}(\omega_i^2-p_i^2)-\{\rho^{(0)}_{i\,i}R_i^2+2\rho^{(0)}_{i\,j}R_j^2+(\beta^{(0)}F^2)_i\}\right]R_i\\ &\qquad=\frac{2R_iR_j}{\kappa_i}\{(\beta^{(2)}F)_{ij}\cos(2\delta_i+\delta_j)+(\beta^{(2)}F)'_{i\,j}\sin(2\delta_i+\delta_j)\}\\ &2c_i\omega_iR_i=\frac{2R_iR_j}{\kappa_i}\{(\beta^{(2)}F)_{i\,j}\sin(2\delta_i+\delta_j)-(\beta^{(2)}F)'_{i\,j}\cos(2\delta_i+\delta_j)\}\\ &\left[\frac{1}{n_j}(\omega_j^2-p_j^2)-\{\rho^{(0)}_{j\,j}R^2+2\rho^{(0)}_{j\,i}R_i^2+(\beta^{(0)}F^2)_j\}\right]R_j\\ &\qquad=\frac{R_i^2}{\kappa_j}\{(\beta^{(2)}F)_{ij}\cos(2\delta_i+\delta_j)+(\beta^{(2)}F)'_{i\,j}\sin(2\delta_i+\delta_j)\}\\ &2c_j\omega_jR_j=\frac{R_i^2}{\kappa_j}\{(\beta^{(2)}F)_{ij}\sin(2\delta_i+\delta_j)-(\beta^{(2)}F)'_{i\,j}\cos(2\delta_i+\delta_j)\}\end{aligned}\right\}\tag{3.26}$$

(d) Oscillations of $\omega=2\omega_i-\omega_k \fallingdotseq 2p_i-p_k$ $(i=1, 2, k=3, 4)$

$$
\begin{aligned}
&\left[\frac{1}{n_i}(\omega_i^2-p_i^2)-\{\rho^{(0)}_{i\,i}R_i^2+2\rho^{(0)}_{i\,k}R_k^2+(\beta^{(0)}F^2)_i\}\right]R_i \\
&\qquad=\frac{2R_iR_k}{\kappa_i}\{(\beta^{(0)}F)_{iik}\cos(2\delta_i-\delta_k)-(\beta^{(0)}F)'_{iik}\sin(2\delta_i-\delta_k)\} \\
&2c_i\omega_iR_i=\frac{2R_iR_k}{\kappa_i}\{(\beta^{(0)}F)_{iik}\sin(2\delta_i-\delta_k)+(\beta^{(0)}F)'_{iik}\cos(2\delta_i-\delta_k)\} \\
&\left[\frac{1}{n_k}(\omega_k^2-p_k^2)-\{\rho^{(0)}_{k\,k}R_k^2+2\rho^{(0)}_{k\,i}R_i^2+(\beta^{(0)}F^2)_k\}\right]R_k \\
&\qquad=\frac{R_i^2}{\kappa_k}\{(\beta^{(0)}F)_{iik}\cos(2\delta_i-\delta_k)-(\beta^{(0)}F)'_{iik}\sin(2\delta_i-\delta_k)\} \\
&2c_k\omega_kR_k=\frac{R_i^2}{\kappa_k}\{-(\beta^{(0)}F)_{iik}\sin(2\delta_i-\delta_k)-(\beta^{(0)}F)'_{iik}\cos(2\delta_i-\delta_k)\}
\end{aligned}
\qquad (3.27)
$$

(e) Oscillations of $\omega=\omega_i-2\omega_k \fallingdotseq p_i-2p_k$ $(i=1, 2, k=3, 4)$

$$
\begin{aligned}
&\left[\frac{1}{n_i}(\omega_i^2-p_i^2)-\{\rho^{(0)}_{i\,i}R_i^2+2\rho^{(0)}_{i\,k}R_k^2+(\beta^{(0)}F^2)_i\}\right]R_i \\
&\qquad=\frac{R_k^2}{\kappa_i}\{(\beta^{(2)}F)_{ikk}\cos(\delta_i-2\delta_k)-(\beta^{(2)}F)'_{ikk}\sin(\delta_i-2\delta_k)\} \\
&2c_i\omega_iR_i=\frac{R_k^2}{\kappa_i}\{(\beta^{(2)}F)_{ikk}\sin(\delta_i-2\delta_k)+(\beta^{(2)}F)'_{ikk}\cos(\delta_i-2\delta_k)\} \\
&\left[\frac{1}{n_k}(\omega_k^2-p_k^2)-\{\rho^{(0)}_{k\,k}R_k^2+2\rho^{(0)}_{k\,i}R_i^2+(\beta^{(0)}F^2)_k\}\right]R_k \\
&\qquad=\frac{2R_iR_k}{\kappa_k}\{(\beta^{(2)}F)_{ikk}\cos(\delta_i-2\delta_k)-(\beta^{(2)}F)'_{ikk}\sin(\delta_i-2\delta_k)\} \\
&2c_k\omega_kR_k=\frac{2R_iR_k}{\kappa_k}\{-(\beta^{(2)}F)_{ikk}\sin(\delta_i-2\delta_k)-(\beta^{(2)}F)'_{ikk}\cos(\delta_i-2\delta_k)\}
\end{aligned}
\qquad (3.28)
$$

(f) Oscillations of $\omega=-2\omega_k-\omega_l \fallingdotseq -2p_k-p_l$ $(k, l=3, 4, k\neq l)$

$$
\begin{aligned}
&\left[\frac{1}{n_k}(\omega_k^2-p_k^2)-\{\rho^{(0)}_{k\,k}R_k^2+2\rho^{(0)}_{k\,l}R_l^2+(\beta^{(0)}F^2)_k\}\right]R_k \\
&\qquad=\frac{2R_kR_l}{\kappa_k}\{(\beta^{(4)}F)_{kl}\cos(2\delta_k+\delta_l)+(\beta^{(4)}F)'_{k\,l}\sin(2\delta_k+\delta_l)\} \\
&2c_k\omega_kR_k=\frac{2R_kR_l}{\kappa_k}\{(\beta^{(4)}F)_{kl}\sin(2\delta_k+\delta_l)-(\beta^{(4)}F)'_{k\,l}\cos(2\delta_k+\delta_l)\}
\end{aligned}
\qquad (3.29)
$$

$$\left[\frac{1}{n_l}(\omega_l^2-p_l^2)-\{\rho^{(0)}_{ll}R_l^2+2\rho^{(0)}_{lk}R_k^2+(\beta^{(0)}F^2)_l\}\right]R_l$$
$$=\frac{R_k^2}{\kappa_l}\{(\beta^{(4)}F)_{kl}\cos(2\delta_k+\delta_l)+(\beta^{(4)}F)'_{kl}\sin(2\delta_k+\delta_l)\}$$
$$2c_l\omega_lR_l=\frac{R_k^2}{\kappa_l}\{(\beta^{(4)}F)_{kl}\sin(2\delta_k+\delta_l)-(\beta^{(4)}F)'_{kl}\cos(2\delta_k+\delta_l)\}$$

C. Summed-and-differential harmonic oscillations consisting of three vibrations

(g) Oscillations of $\omega=\omega_1+\omega_2-\omega_k\fallingdotseq p_1+p_2-p_k$ $(k=3, 4)$

$$\left[\frac{1}{n_1}(\omega_1^2-p_1^2)-\{\rho^{(0)2}_{11}R_1^2+2\rho^{(0)}_{12}R_2^2+2\rho^{(0)}_{1k}R_k^2+(\beta^{(0)}F^2)_1\}\right]R_1$$
$$=\frac{2R_2R_k}{\kappa_1}\{(\beta^{(0)}F)_{12k}\cos(\delta_1+\delta_2-\delta_k)-(\beta^{(0)}F)'_{12k}\sin(\delta_1+\delta_2-\delta_k)\}$$
$$2c_1\omega_1R_1=\frac{2R_2R_k}{\kappa_1}\{(\beta^{(0)}F)_{12k}\sin(\delta_1+\delta_2-\delta_k)+(\beta^{(0)}F)'_{12k}\cos(\delta_1+\delta_2-\delta_k)\}$$
$$\left[\frac{1}{n_2}(\omega_2^2-p_2^2)-\{\rho^{(0)}_{22}R_2^2+2\rho^{(0)}_{21}R_1^2+2\rho^{(0)}_{2k}R_k^2+(\beta^{(0)}R^2)_2\}\right]R_2$$
$$=\frac{2R_1R_k}{\kappa_2}\{(\beta^{(0)}F)_{12k}\cos(\delta_1+\delta_2-\delta_k)-(\beta^{(0)}F)'_{12k}\sin(\delta_1+\delta_2-\delta_k)\}$$
$$2c_2\omega_2R_2=\frac{2R_1R_k}{\kappa_2}\{(\beta^{(0)}F)_{12k}\sin(\delta_1+\delta_2-\delta_k)+(\beta^{(0)}F)'_{12k}\cos(\delta_1+\delta_2-\delta_k)\}$$
$$\left[\frac{1}{n_k}(\omega_k^2-p_k^2)-\{\rho^{(0)}_{kk}R_k^2+2\rho^{(0)}_{k1}R_1^2+2\rho^{(0)}_{k2}R_2^2+(\beta^{(0)}F^2)_k\}\right]R_k$$
$$=\frac{2R_1R_2}{\kappa_k}\{(\beta^{(0)}F)_{12k}\cos(\delta_1+\delta_2-\delta_k)-(\beta^{(0)}F)'_{12k}\sin(\delta_1+\delta_2-\delta_k)\}$$
$$2c_k\omega_kR_k=\frac{2R_1R_2}{\kappa_k}\{-(\beta^{(0)}F)_{12k}\sin(\delta_1+\delta_2-\delta_k)-(\beta^{(0)}F)'_{12k}\cos(\delta_1+\delta_2-\delta_k)\}$$

(3. 30)

(h) Oscillations of $\omega=\omega_i-\omega_3-\omega_4\fallingdotseq p_i-p_3-p_4$ $(i=1, 2)$

$$\left[\frac{1}{n_i}(\omega_i^2-p_i^2)-\{\rho^{(0)}_{ii}R_i^2+2\rho^{(0)}_{i3}R_3^2+2\rho^{(0)}_{i4}R_4^2+(\beta^{(0)}F^2)_i\}\right]R_i$$
$$=\frac{2R_3R_4}{\kappa_i}\{(\beta^{(2)}F)_{i34}\cos(\delta_i-\delta_3-\delta_4)-(\beta^{(2)}F)'_{i34}\sin(\delta_i-\delta_3-\delta_4)\}$$
$$2c_i\omega_iR_i=\frac{2R_3R_4}{\kappa_i}\{(\beta^{(2)}F)_{i34}\sin(\delta_i-\delta_3-\delta_4)+(\beta^{(2)}F)'_{34}\cos(\delta_i-\delta_3-\delta_4)\}$$

$$
\begin{aligned}
&\left[\frac{1}{n_3}(\omega_3^2-p_3^2)-\{\rho_{33}^{(0)}R_3^2+2\rho_{3i}^{(0)}R_i^2+2\rho_{34}^{(0)}R_4^2+(\beta^{(0)}F^2)_3\}\right]R_3\\
&\qquad=\frac{2R_iR_4}{\kappa_3}\{(\beta^{(2)}F)_{i34}\cos(\delta_i-\delta_3-\delta_4)-(\beta^{(2)}F)'_{i40}\sin(\delta_i-\delta_3-\delta_4)\}\\
&2c_3\omega_3R_3=\frac{2R_iR_4}{\kappa_3}\{-(\beta^{(2)}F)_{i34}\sin(\delta_i-\delta_3-\delta_4)-(\beta^{(2)}F)'_{i34}\cos(\delta_i-\delta_3-\delta_4)\}\\
&\left[\frac{1}{n_4}(\omega_4^2-p_4^2)-\{\rho_{44}^{(0)}R_4^2+2\rho_{4i}^{(0)}R_i^2+2\rho_{43}^{(0)}R_3^2+(\beta^{(0)}F^2)_4\}\right]R_4\\
&\qquad=\frac{2R_iR_3}{\kappa_4}\{(\beta^{(2)}F)_{i34}\cos(\delta_i-\delta_3-\delta_4)-(\beta^{(2)}F)'_{i34}\sin(\delta_i-\delta_3-\delta_4)\}\\
&2c_4\omega_4R_4=\frac{2R_iR_3}{\kappa_4}\{-(\beta^{(2)}F)_{i34}\sin(\delta_i-\delta_3-\delta_4)-(\beta^{(2)}F)'_{i34}\cos(\delta_i-\delta_3-\delta_4)\}
\end{aligned}
\tag{3.31}
$$

In Eqs. (3.24)$\sim$(3.31), the coefficients n_i and $\rho_{ij}^{(0)}$, $(\beta^{(0)}F^2)_i$ are given by Eqs. (3.12) and (3.23), and other coefficients are

$$
\begin{aligned}
&(\beta^{(2)}F)_{ij}=\xi_{ij}^{(2)}F_1-\eta_{ij}^{(2)}F_2+\zeta_{ij}^{(2)}F_3-\mu_{ij}^{(2)}F_4\\
&(\beta^{(2)}F)'_{ij}=\eta_{ij}^{(2)}F_1+\xi_{ij}^{(2)}F_2+\mu_{ij}^{(2)}F_3+\zeta_{ij}^{(2)}F_4\\
&\xi_{ij}^{(2)}=2\{3\beta_{40c}^{(2)}+(2\kappa_i+\kappa_j)\beta_{31c}^{(2)}+\kappa_i(\kappa_i+2\kappa_j)\beta_{22c}^{\prime(2)}+3\kappa_i^2\kappa_j\beta_{13c}^{\prime(2)}\}\\
&\eta_{ij}^{(2)}=2\{3\beta_{40s}^{(2)}+(2\kappa_i+\kappa_j)\beta_{31s}^{(2)}+\kappa_i(\kappa_i+2\kappa_j)\beta_{22s}^{\prime(2)}+3\kappa_i^2\kappa_j\beta_{13s}^{\prime(2)}\}\\
&\zeta_{ij}^{(2)}=2\{3\beta_{31c}^{\prime(2)}+(2\kappa_i+\kappa_j)\beta_{22c}^{(2)}+\kappa_i(\kappa_i+2\kappa_j)\beta_{13c}^{(2)}+3\kappa_i^2\kappa_j\beta_{04c}^{(2)}\}\\
&\mu_{ij}^{(2)}=2\{3\beta_{31s}^{\prime(2)}+(2\kappa_i+\kappa_j)\beta_{22s}^{(2)}+\kappa_i(\kappa_i+2\kappa_j)\beta_{13s}^{(2)}+3\kappa_i^2\kappa_j\beta_{04s}^{(2)}\}\\
&\qquad(i,\ j=1,\ 2)
\end{aligned}
\tag{3.32}
$$

$$
\begin{aligned}
&(\beta^{(4)}F)_{kl}=\xi_{kl}^{(4)}F_1+\eta_{kl}^{(4)}F_2+\zeta_{kl}^{(4)}F_3+\mu_{kl}^{(4)}F_4\\
&(\beta^{(4)}F)'_{kl}=\eta_{kl}^{(4)}F_1-\xi_{kl}^{(4)}F_2+\mu_{kl}^{(4)}F_3-\zeta_{kl}^{(4)}F_4\\
&\xi_{kl}^{(4)}=2\{12\beta_{40c}^{(4)}+3(2\kappa_k+\kappa_l)\beta_{31c}^{(4)}+2\kappa_k(\kappa_k+2\kappa_l)\beta_{22c}^{(4)}+3\kappa_k^2\kappa_l\beta_{13c}^{(4)}\}\\
&\eta_{kl}^{(4)}=2\{12\beta_{40s}^{(4)}+3(2\kappa_k+\kappa_l)\beta_{31s}^{(4)}+2\kappa_k(\kappa_k+2\kappa_l)\beta_{22s}^{(4)}+3\kappa_k^2\kappa_l\beta_{13s}^{(4)}\}\\
&\zeta_{kl}^{(4)}=2\{3\beta_{31c}^{(4)}+2(2\kappa_k+\kappa_l)\beta_{22c}^{(4)}+3\kappa_k(\kappa_k+2\kappa_l)\beta_{13c}^{(4)}+12\kappa_k^2\kappa_l\beta_{04c}^{(4)}\}\\
&\mu_{kl}^{(4)}=2\{3\beta_{31s}^{(4)}+2(2\kappa_k+\kappa_l)\beta_{22s}^{(4)}+3\kappa_k(\kappa_k+2\kappa_l)\beta_{13s}^{(4)}+12\kappa_k^2\kappa_l\beta_{04s}^{(4)}\}\\
&\qquad(k,\ l=3,\ 4)
\end{aligned}
\tag{3.33}
$$

$$
\begin{aligned}
&(\beta^{(0)}F)_{ijk}=\xi^{(0)}_{ijk}F_1+\eta^{(0)}_{ijk}F_2+\zeta^{(0)}_{ijk}F_3-\mu^{(0)}_{ijk}F_4\\
&(\beta^{(0)}F)'_{ijk}=\eta^{(0)}_{ijk}F_1-\xi^{(0)}_{ijk}F_2-\mu^{(0)}_{ijk}F_3-\zeta^{(0)}_{ijk}F_4\\
&\xi^{(0)}_{ijk}=2\{4\beta^{(0)}_{40}+(\kappa_i+\kappa_j+\kappa_k)\beta^{(0)}_{31c}+\kappa_k(\kappa_i+\kappa_j)\beta^{(0)}_{22}+2\kappa_i\kappa_j\beta^{(0)}_{22c}+\kappa_i\kappa_j\kappa_k\beta^{(0)}_{13c}\}\\
&\eta^{(0)}_{ijk}=2\{(\kappa_i+\kappa_j-\kappa_k)\beta^{(0)}_{31s}+2\kappa_i\kappa_j\beta^{(0)}_{22s}-\kappa_i\kappa_j\kappa_k\beta^{(0)}_{13s}\}\\
&\zeta^{(0)}_{ijk}=2\{\beta^{(0)}_{31c}+(\kappa_i+\kappa_j)\beta^{(0)}_{22}+2\kappa_k\beta^{(0)}_{22c}+(\kappa_i\kappa_j+\kappa_j\kappa_k+\kappa_k\kappa_i)\beta^{(0)}_{13c}+4\kappa_i\kappa_j\kappa_k\beta^{(0)}_{04}\}\\
&\mu^{(0)}_{ijk}=2\{\beta^{(0)}_{31s}+2\kappa_k\beta^{(0)}_{22s}+(\kappa_i\kappa_j-\kappa_j\kappa_k-\kappa_k\kappa_i)\beta^{(0)}_{13s}\}\\
&\qquad(i,\ j=1,\ 2;\ k=3,\ 4)
\end{aligned}
\tag{3.34}
$$

$$
\begin{aligned}
&(\beta^{(2)}F)_{ikl}=\xi^{(2)}_{ikl}F_1+\eta^{(2)}_{ikl}F_2+\zeta^{(2)}_{ikl}F_3+\mu^{(2)}_{ikl}F_4\\
&(\beta^{(2)}F)'_{ikl}=\eta^{(2)}_{ikl}F_1-\xi^{(2)}_{ikl}F_2+\mu^{(2)}_{ikl}F_3-\zeta^{(2)}_{ikl}F_4\\
&\xi^{(2)}_{ikl}=2\{3\beta^{(2)}_{40c}+(\kappa_k+\kappa_l)\beta^{(2)}_{31c}+3\kappa_i\beta'^{(2)}_{31c}+\kappa_i(\kappa_k+\kappa_l)\beta^{(2)}_{22c}+\kappa_k\kappa_l\beta'^{(2)}_{22c}+\kappa_i\kappa_k\kappa_l\beta^{(2)}_{13c}\}\\
&\eta^{(2)}_{ikl}=2\{3\beta^{(2)}_{40s}+(\kappa_k+\kappa_l)\beta^{(2)}_{31s}+3\kappa_i\beta'^{(2)}_{31s}+\kappa_i(\kappa_k+\kappa_l)\beta^{(2)}_{22s}+\kappa_k\kappa_l\beta'^{(2)}_{22s}+\kappa_i\kappa_k\kappa_l\beta^{(2)}_{13s}\}\\
&\zeta^{(2)}_{ikl}=2\{\beta^{(2)}_{31c}+\kappa_i\beta^{(2)}_{22c}+(\kappa_k+\kappa_l)\beta'^{(2)}_{22c}+\kappa_i(\kappa_k+\kappa_l)\beta^{(2)}_{13c}+3\kappa_k\kappa_l\beta'^{(2)}_{13c}+3\kappa_i\kappa_k\kappa_l\beta^{(2)}_{04c}\}\\
&\mu^{(2)}_{ikl}=2\{\beta^{(2)}_{31s}+\kappa_i\beta^{(2)}_{22s}+(\kappa_k+\kappa_l)\beta'^{(2)}_{22s}+\kappa_i(\kappa_k+\kappa_l)\beta^{(2)}_{13s}+3\kappa_k\kappa_l\beta'^{(2)}_{13s}+3\kappa_i\kappa_k\kappa_l\beta^{(2)}_{04s}\}\\
&\qquad(i=1,\ 2;\ k,\ l=3,\ 4)
\end{aligned}
\tag{3.35}
$$

Eq. (3.32) is applied to Eqs. (3.24) and (3.26), Eq. (3.33) to Eqs. (3.25) and (3.29), Eq. (3.34) to Eqs. (3.27) and (3.30), and Eq. (3.35) to Eqs. (3.28) and (3.31).

Equations for amplitudes, frequencies, and phase angles can be derived from Eqs. (3.24)～(3.31) by the similar procedure as in the reports (6), (13), (14), and (15). Since Eqs. (3.24)～(3.31) are similar to those in the previous papers, the shapes of resonance curves are similar to those shown in the previous papers (14) and (15).

It can easily be proved that for the oscillations of Eqs. (3.27) and (3.30) to occur, the component N(0) is required; for those of Eqs. (3.24), (3.26), (3.28), and (3.31), both N(0) and N(2) are required; and finally, for oscillations of Eqs. (3.25) and (3.29). both N(0) and N(4) are necessary.

II. Forced oscillations caused by unsymmetrical nonlinear spring characteristics

A. Subharmonic oscillations of order 1/2

(a) Oscillations of $\omega=2\omega_i\fallingdotseq 2p_i$ $(i=1,\ 2)$

$$\left.\begin{aligned}\frac{1}{n_i}\left(\frac{1}{4}\omega^2-p_i^2\right)-\{\rho_{ii}^{(0)}R_i^2+(\beta^{(0)}F^2)_i\}&=\frac{1}{\kappa_i}\{(\varepsilon^{(1)}F)_{ii}\cos 2\delta_i+(\varepsilon^{(1)}F)'_{ii}\sin 2\delta_i\}\\ c_i\omega&=\frac{1}{\kappa_i}\{(\varepsilon^{(1)}F)_{ii}\sin 2\delta_i-(\varepsilon^{(1)}F)'_{ii}\cos 2\delta_i\}\end{aligned}\right\}\tag{3.36}$$

(b) Oscillations of $\omega=-2\omega_k\doteqdot -2p_k$ $(k=3,\ 4)$

$$\left.\begin{aligned}\frac{1}{n_k}\left(\frac{1}{4}\omega^2-p_k^2\right)-\{\rho_{kk}^{(0)}R_k^2+(\beta^{(0)}F^2)_k\}&=\frac{1}{\kappa_k}\{(\varepsilon^{(3)}F)_{kk}\cos 2\delta_k+(\varepsilon^{(3)}F)'_{kk}\sin 2\delta_k\}\\ c_k\omega&=\frac{1}{\kappa_k}\{-(\varepsilon^{(3)}F)_{kk}\sin 2\delta_k+(\varepsilon^{(3)}F)'_{kk}\cos 2\delta_k\}\end{aligned}\right\}\tag{3.37}$$

B. Summed-and-differential harmonic oscillations

(c) Oscillations of $\omega=\omega_1+\omega_2\doteqdot p_1+p_2$

$$\left.\begin{aligned}\left[\frac{1}{n_1}(\omega_1^2-p_1^2)-\{\rho_{11}^{(0)}R_1^2+2\rho_{12}^{(0)}R_2^2+(\beta^{(0)}F^2)_1\}\right]R_1&\\ =\frac{R_2}{\kappa_1}\{(\varepsilon^{(1)}F)_{12}\cos(\delta_1+\delta_2)+(\varepsilon^{(1)}F)'_{12}\sin(\delta_1+\delta_2)\}&\\ 2c_1\omega_1R_1=\frac{R_2}{\kappa_1}\{(\varepsilon^{(1)}F)_{12}\sin(\delta_1+\delta_2)-(\varepsilon^{(1)}F)'_{12}\cos(\delta_1+\delta_2)\}&\\ \left[\frac{1}{n_2}(\omega_2^2-p_2^2)-\{\rho_{22}^{(0)}R_2^2+2\rho_{21}^{(0)}R_1^2+(\beta^{(0)}F^2)_2\}\right]R_2&\\ =\frac{R_1}{\kappa_2}\{(\varepsilon^{(1)}F)_{21}\cos(\delta_1+\delta_2)+(\varepsilon^{(1)}F)'_{21}\sin(\delta_1+\delta_2)\}&\\ 2c_2\omega_2R_2=\frac{R_1}{\kappa_2}\{(\varepsilon^{(1)}F)_{21}\sin(\delta_1+\delta_2)-(\varepsilon^{(1)}F)'_{21}\cos(\delta_1+\delta_2)\}&\end{aligned}\right\}\tag{3.38}$$

(d) Oscillations of $\omega=\omega_i-\omega_k\doteqdot p_i-p_k$ $(i=1,\ 2;\ k=3,\ 4)$

$$\left.\begin{aligned}\left[\frac{1}{n_i}(\omega_i^2-p_i^2)-\{\rho_{ii}^{(0)}R_i^2+2\rho_{ik}^{(0)}R_k^2+(\beta^{(0)}F^2)_i\}\right]R_i&\\ =\frac{R_k}{\kappa_i}\{(\varepsilon^{(1)}F)''_{ik}\cos(\delta_i-\delta_k)-(\varepsilon^{(1)}F)'''_{ik}\sin(\delta_i-\delta_k)\}&\\ 2c_i\omega_iR_i=\frac{R_k}{\kappa_i}\{(\varepsilon^{(1)}F)''_{ik}\sin(\delta_i-\delta_k)+(\varepsilon^{(1)}F)'''_{ik}\cos(\delta_i-\delta_k)\}&\\ \left[\frac{1}{n_k}(\omega_k^2-p_k^2)-\{\rho_{kk}^{(0)}R_k^2+2\rho_{ki}^{(0)}R_i^2+(\beta^{(0)}F^2)_k\}\right]R_k&\end{aligned}\right\}\tag{3.39}$$

$$
\left.
\begin{aligned}
&= \frac{R_i}{\kappa_k}\{(\varepsilon^{(1)}F)''_{ik}\cos(\delta_i-\delta_k)-(\varepsilon^{(1)}F)'''_{ik}\sin(\delta_i-\delta_k)\} \\
2c_k\omega_k R_k &= \frac{R_i}{\kappa_k}\{-(\varepsilon^{(1)}F)''_{ik}\sin(\delta_i-\delta_k)-(\varepsilon^{(1)}F)'''_{ik}\cos(\delta_i-\delta_k)\}
\end{aligned}
\right\}
$$

(e) Oscillations of $\omega=-\omega_3-\omega_4\fallingdotseq -p_3-p_4$

$$
\left.
\begin{aligned}
&\left[\frac{1}{n_3}(\omega_3^2-p_3^2)-\{\rho_{33}^{(0)}R_3^2+2\rho_{34}^{(0)}R_4^2+(\beta^{(0)}F^2)_3\}\right]R_3 \\
&\qquad = \frac{R_4}{\kappa_3}\{(\varepsilon^{(3)}F)_{34}\cos(\delta_3+\delta_4)+(\varepsilon^{(3)}F)'_{34}\sin(\delta_3+\delta_4)\} \\
&2c_3\omega_3 R_3 = \frac{R_4}{\kappa_3}\{(\varepsilon^{(3)}F)_{34}\sin(\delta_3+\delta_4)-(\varepsilon^{(3)}F)'_{34}\cos(\delta_3+\delta_4)\} \\
&\left[\frac{1}{n_4}(\omega_4^2-p_4^2)-\{\rho_{44}^{(0)}R_4^2+2\rho_{43}^{(0)}R_3^2+(\beta^{(0)}F^2)_4\}\right]R_4 \\
&\qquad = \frac{R_3}{\kappa_4}\{(\varepsilon^{(3)}F)_{43}\cos(\delta_3+\delta_4)+(\varepsilon^{(3)}F)'_{43}\sin(\delta_3+\delta_4)\} \\
&2c_4\omega_4 R_4 = \frac{R_3}{\kappa_4}\{(\varepsilon^{(3)}F)_{43}\sin(\delta_3+\delta_4)-(\varepsilon^{(3)}F)'_{43}\cos(\delta_3+\delta_4)\}
\end{aligned}
\right\} \quad (3.40)
$$

The coefficients of Eqs. (3.36)~(3.40) are as follows:

$$
\left.
\begin{aligned}
(\varepsilon^{(1)}F)_{ij} &= \lambda_{ij}^{(1)}F_1-\sigma_{ij}^{(1)}F_2+\tau_{ij}^{(1)}F_3-\nu_{ij}^{(1)}F_4 \\
(\varepsilon^{(1)}F)'_{ij} &= \sigma_{ij}^{(1)}F_1+\lambda_{ij}^{(1)}F_2+\nu_{ij}^{(1)}F_3+\tau_{ij}^{(1)}F_4 \\
\lambda_{ij}^{(1)} &= 4\varepsilon_{30c}^{(1)}+2(\kappa_i+\kappa_j)\varepsilon_{21c}^{(1)}+4\kappa_i\kappa_j\varepsilon_{12c}^{\prime(1)} \\
\sigma_{ij}^{(1)} &= 4\varepsilon_{30s}^{(1)}+2(\kappa_i+\kappa_j)\varepsilon_{21s}^{(1)}+4\kappa_i\kappa_j\varepsilon_{12s}^{\prime(1)} \\
\tau_{ij}^{(1)} &= 4\varepsilon_{21c}^{\prime(1)}+2(\kappa_i+\kappa_j)\varepsilon_{12c}^{(1)}+4\kappa_i\kappa_j\varepsilon_{03c}^{(1)} \\
\nu_{ij}^{(1)} &= 4\varepsilon_{21s}^{\prime(1)}+2(\kappa_i+\kappa_j)\varepsilon_{12s}^{(1)}+4\kappa_i\kappa_j\varepsilon_{03s}^{(1)} \\
&\qquad (i,\ j=1,\ 2)
\end{aligned}
\right\} \quad (3.41)
$$

$$
\left.
\begin{aligned}
(\varepsilon^{(1)}F)''_{ik} &= \lambda_{ik}^{\prime(1)}F_1+\sigma_{ik}^{\prime(1)}F_2+\tau_{ik}^{\prime(1)}F_3+\nu_{ik}^{\prime(1)}F_4 \\
(\varepsilon^{(1)}F)'''_{ik} &= \sigma_{ik}^{\prime(1)}F_1-\lambda_{ik}^{\prime(1)}F_2+\nu_{ik}^{\prime(1)}F_3-\tau_{ik}^{\prime(1)}F_4 \\
\lambda_{ik}^{\prime(1)} &= 4\varepsilon_{30c}^{(1)}+4\kappa_i\varepsilon_{21c}^{\prime(1)}+2\kappa_k\varepsilon_{21c}^{(1)}+2\kappa_i\kappa_k\varepsilon_{12c}^{(1)} \\
\sigma_{ik}^{\prime(1)} &= 4\varepsilon_{30s}^{(1)}+4\kappa_i\varepsilon_{21s}^{\prime(1)}+2\kappa_k\varepsilon_{21s}^{(1)}+2\kappa_i\kappa_k\varepsilon_{12s}^{(1)} \\
\tau_{ik}^{\prime(1)} &= 2\varepsilon_{21c}^{(1)}+2\kappa_i\varepsilon_{12c}^{(1)}+4\kappa_k\varepsilon_{12c}^{\prime(1)}+4\kappa_i\kappa_k\varepsilon_{03c}^{(1)} \\
\nu_{ik}^{\prime(1)} &= 2\varepsilon_{21s}^{(1)}+2\kappa_i\varepsilon_{12s}^{(1)}+4\kappa_k\varepsilon_{12s}^{\prime(1)}+4\kappa_i\kappa_k\varepsilon_{03s}^{(1)} \\
&\qquad (i=1,\ 2;\ k=3,\ 4)
\end{aligned}
\right\} \quad (3.42)
$$

$$
\left.\begin{aligned}
(\varepsilon^{(3)}F)_{kl} &= \lambda^{(3)}_{kl}F_1+\sigma^{(3)}_{kl}F_2+\tau^{(3)}_{kl}F_3+\nu^{(3)}_{kl}F_4\\
(\varepsilon^{(3)}F)'_{kl} &= \sigma^{(3)}_{kl}F_1-\lambda^{(3)}_{kl}F_2+\nu^{(3)}_{kl}F_3-\tau^{(3)}_{kl}F_4\\
\lambda^{(3)}_{kl} &= 4\{3\varepsilon^{(3)}_{30c}+(\kappa_k+\kappa_l)\varepsilon^{(3)}_{21c}+\kappa_k\kappa_l\varepsilon^{(3)}_{12c}\}\\
\sigma^{(3)}_{kl} &= 4\{3\varepsilon^{(3)}_{30s}+(\kappa_k+\kappa_l)\varepsilon^{(3)}_{21s}+\kappa_k\kappa_l\varepsilon^{(3)}_{12s}\}\\
\tau^{(3)}_{kl} &= 4\{\varepsilon^{(3)}_{21c}+(\kappa_k+\kappa_l)\varepsilon^{(3)}_{12c}+3\kappa_k\kappa_l\varepsilon^{(3)}_{03c}\}\\
\nu^{(3)}_{kl} &= 4\{\omega^{(3)}_{21s}+(\kappa_k+\kappa_l)\varepsilon^{(3)}_{12s}+3\kappa_k\kappa_l\varepsilon^{(3)}_{03s}\}\\
&\qquad (k,\ l=3,\ 4)
\end{aligned}\right\} \qquad (3.43)
$$

Eq. (3.41) is applied to Eqs. (3.36) and (3.38), Eq. (3.42) to Eq. (3.39), and Eq. (3.43) to Eqs. (3.37) and (3.40). For oscillations of Eqs. (3.36), (3.38), and (3.39) to occur, both the components N(0) anp N(1) are required; for those of Eqs. (3.37) and (3.40), both N(0) and N(3) are necessary.

Since Eqs. (3.36)~(3.40) are similar to those in the papers (10), (14), and (18), the shapes of resonance curves given by Eqs. (3.36)~(3.40) are similar to those shown in the paper (14).

The required components of nonlinear characteristics for the occurrences of oscillations are shown in Table 3.1. It can be seen that the isotropic component N(0) is necessary for all kinds of nonlinear forced oscillations.

3. 5. Comparisons with the experimental results

Since the relationship $p_1 > i_p\,\omega \fallingdotseq 2\omega$ holds in the previous chapter (the paper (8)) and the previous papers (2), (4), (5), the relationships containing p_1 in Table 3.1 cannot hold and hence oscillations in which p_1 is concerned cannot take place. Concequently, oscillations anticipated to occur in the experimental apparatus of the previous papers are restricted within those shown in Table 3.2.

In the experimental apparatus, nonlinear characteristics are induced by angular clearances in single-row deep groove ball bearings. In the system treated in the papers (2), (4) and (5), the equilibrium position of the shaft deviates slightly from the center of the angular clearance, and in that treated in the previous chapter (the paper (8)), it located almost at the center of it. Accordingly, unsymmetrical nonlinear characteristics appear somewhat predominantly in the former, while symmetrical ones appear somewhat predominantly in the latter. Furthermore, in the previous chapter (the paper (8)), experiments are performed for both case Ⅰ, where there is no anisotropy in nonlinear characteristics, and case Ⅲ, where the anisotropy exists. It is easily seen that the strong nonlinear components N(3) and N(4) are not expected.

The experimental results in the previous papers can be easily explained as follows by the analytical results obtained in the present chapter. (cf. Table 3.2):

(i) In the papers (2), (4), and (5), forced oscillations caused by symmetrical nonlinear characteristics do not take place because of small N(0).

(ii) In the papers (2), (4), and (5), forced oscillations induced by the the component N(1) of unsymmetrical nonlinear characteristics which is considered to be large take place strongly, and oscillations caused by N(3) appear only with small amplitude or not at all.

Table 3. 2. Experimental results about the occurrences of nonlinear forced oscillations

Kinds of oscillations		Forced oscillations caused by symmetrical nonlinear characteristics						Forced oscillations caused by unsymmetrical nonlinear characteristics			
		Subharmonic oscillations of order 1/3		Summed-and-differential harmonic oscillations				Subharmonic oscillations of order 1/2		Summed-and-differential harmonic oscillations	
		$3p_2$	$-3p_3$ $-3p_4$	$2p_2-p_3$ $2p_2-p_4$	p_2-2p_3 p_2-2p_4	$-2p_3-p_4$ $-p_3-2p_4$	$p_2-p_3-p_4$	$2p_2$	$-2p_3$ $-2p_4$	p_2-p_3 p_2-p_4	$-p_3-p_4$
Necessary nonlinear components		N(0) N(2)	N(0) N(4)	N(0) only	N(0) N(2)	N(0) N(4)	N(0) N(2)	N(0) N(1)	N(0) N(3)	N(0) N(1)	N(0) N(3)
The papers (4), (5), (6)		×	×	×	×	×	×	○	△	○	△
The paper (2)	Ⅰ	×	×	○	×	×	×	○	×	○	×
	Ⅱ	○	×	○	○	×	○	○	×	○	×

○ : always occur, × : never occur, △ : not occur or appear with small amplitudes depending on assembly,

The papers (4), (5), (6) : The systems have large unsymmetrical nonlinear charcteristics.

The paper (2) : The systems have large symmetrical nonlinear characteristics

Ⅰ : isotropic symmetrical nonlinear characteristics

Ⅱ : anisotropic symmetrical nonlinear characteristics

(iii) In the previous chapter (the paper (8)), all oscillations requiring N(3) do not appear because of the small unsymmetrical nonlinear characteristics.

(iv) In case Ⅰ of the previous chapter (the paper (8)), oscillations of $2p_2-p_3$ and $2p_2-p_4$ needing only the isotropic component N(0) can take place, while oscillations requiring also the anisotropic component N(2) cannot appear.

(v) In case Ⅱ of the previous chapter (the paper (8)), in addition to the oscillations requiring only N(0), those needing both N(0) and N(2) take place.

(vi) In both cases Ⅰ and Ⅱ, oscillations requiring N(4) which is considered small cannot appear.

(vii) It can be easily seen from the constitutions of Eqs. (3. 24)～(3. 31) and (3. 36)～(3. 40) that the shapes of the resonance curves are similar to those in the report (14).

(viii) In the previous chapter (the paper (8)) where N(0), and hence the coefficients $\rho_s^{(0)}$ are large, all the resonance curves bend strongly. Consequently ranges where oscillations occur are fairly wide.

3. 6. Conclusions

The results obtained in this chapter are summarized as follows:

(1) Representation of nonlinear spring characteristics through polar coordinates is useful for analytical treatment of the nonlinear forced oscillations of whirling motions.

(2) By adopting polar coordinates, nonlinear spring characteristics are clas-

sified into the constant component N(0) and the components N(1), N(2), N(3), N(4), ... which change their magnitude 1, 2, 3, 4, ... times, respectively, while the shaft whirls around its equilibrium position.

(3) The components N(0), N(2), N(4), ..., N($2n$), ... (n : a positive integer) belong to the symmetrical nonlinear characteristics, and the components N(1), N(3), ..., N($2n+1$), ... belong to the unsymmetrical nonlinear characteristics.

(4) All nonlinear forced oscillations require for their occurrence the isotropic component N(0).

(5) For all nonlinear forced oscillations, the sign of the coefficient of N(0) determines whether resonance curves belong to the hard or soft spring type, and the magnitude of the absolute value of the coefficient of N(0) decides the degree of bending of the resonance curves.

(6) Occurrences of nonlinear forced oscillations require only N(0), or both N(0) and one of N(1)~N(n). And the necessary components are different for each kind of oscillations.

(7) Shapes of resonance curves of nonlinear forced oscillations are similar to those of rectilinear systems in the paper (14) and (15).

(8) By representing nonlinear spring characteristics by polar coordinates as proposed in this chapter, the experimental results obtained in the previous chapter and the previous papers are explained clearly.

(9) By adopting such representations, the relative difficulties of occurrences of oscillations are easily estimated, and the properties of oscillations can be made clear.

References

1) T. Yamamoto and Y. Ishida, "The Particular Vibration Phenomena Due to Ball Bearings at the Major Critical Speed". Bulletin of JSME, Vol. **17**, No. 103 (1974-1), pp. 59-67.
2) T. Yamamoto, "On the Critical Speed of a Shaft of Sub-harmonic Oscillation", Trans. of Japan Soc. of Mech. Engrs., Vol. **21**, No. 111 (1955-11), pp. 853-858.
T. Yamamoto, "On the Vibrations of a Rotating Shaft", Memoirs of the Faculty of Engineering, Nagoya University, Vol. **9**, No. 1 (1957-5), pp. 24-43.
3) T. Yamamoto, "On the Critical Speeds of Synchronous Backward Precession", Trans. of Japan Soc. of Mech. Engrs., Vol. **22**, No. 115 (1956-3), pp. 167-171.
T. Yamamoto, "On the Vibrations of a Rotating Shaft", Memoirs of the Faculty of Engineering, Nagoya University, Vol. **9**, No.1 (1957-5), pp. 71-78.
4) T. Yamamoto, "On the Critical Speeds with Peculiar Modes of Vibration", Trans. of Japan Soc. of Mech. Engrs., Vol. 22, No. 115 (1956-3), pp. 172-177.
T. Yamamoto, "On the Vibrations of a Rotating Shaft", Memoirs of the Faculty of Engineering, Nagoya University, Vol. **9**, No. 1 (1957-5), pp. 43-53.
5) T. Yamamoto, "Response Curves at the Critical Speeds of Sub-Harmonic and "Summed and Differential Harmonic" Oscillations", Bulletin of JSME, Vol. **3**, No. 12 (1960-10), pp. 397-403.
6) T. Yamamoto, "On the Critical Speed of a Shaft at Lower Rotating Speeds", Trans. of Japan Soc. of Mech. Engrs., Vol, **22**, No. 123 (1956-11), pp. 863-867.
T. Yamamoto, "On the Vibrations of a Rotating Shaft", Memoirs of the Faculty of Engineering, Nagoya University, Vol. **9**, No. 1 (1957-5), pp. 79-86.
7) H. D. Taylor, "Critical-Speed Behavior of Unsymmetrical Shafts", Jour. App. Mech. (1940-6), pp. A71-79.
8) T. Yamamoto, Y. Ishida, and J. Kawasumi, "Oscillations of a Rotating Shaft with

Symmetrical Nonlinear Spring Characteristics", Bulletin of JSME, Vol. **18**, No. 123 (1975-9), pp. 965-975.

9) T. Yamamoto, "On Sub-harmonic Oscillations and on Vibrations of Peculiar Modes in Non-linear Systems Having Multiple Degrees of Freedom", Trans. of Japan Soc. of Mech. Engrs., Vol. **22**, No. 123 (1956-11), pp. 868-875.
T. Yamamoto, "On the Vibrations of a Rotating Shaft", Memoirs of the Faculty of Engineering, Nagoya University, Vol. **9**, No. 1 (1957-5), pp. 53-71.

10) T. Yamamoto, "On Sub-Harmonic and "Summed and Differential Harmonic" Oscillations of Rotating Shaft", Bulletion of JSME, Vol. **4**, No. 13 (1961-2), pp. 51-58.

11) T. Nishihara, Y. Sawaragi, and Y. Okada, "On the 1/3 Sub-Harmonic Resonance of the System with Non-Linear Restoring Force", Trans. of Japan Soc. of Mech. Engrs., Vol. **17**, No. 68 (1951), pp. 26-31.

12) K. Nishino, "Some Notes on the Sub-harmonic Resonance in the Non-linear Mechanical Vibratory System", J. Japan Soc. Appl. Mech., Vol. **3**, No. 18 (1950-8), pp. 121-126.

13) T. Yamamoto, ""Summed and Differential Harmonic" Oscillations in Symmetrical Nonlinear Systems", Trans. of Japan Soc. Mech. Engrs., Vol. **27**, No. 182 (1961-10). pp. 1676-1683.
T. Yamamoto and S. Hayashi, "Summed and Differential Harmonic Oscillations in Nonlinear Vibratory Systems", Vol. **18**, No. 2 (1966-11), pp. 124-139.

14) T. Yamamoto and S. Hayashi, "On the Response Curves and the Stability of "Summed and Differential Harmonic" Oscillations", Bulletin of JSME, Vol. **6**, No. 23 (1963-8), pp. 420-429.

15) S. Hayashi, "On the "Summed and Differential Harmonic" Oscillations in Vibratory Systems with Symmetrical Nonlinear Spring Characteristics", Trans. of Japan Soc. Mech. Engrs., Vol. **32**, No. 234 (1966-2), pp. 219-226.
T. Yamamoto and S. Hayashi, "Summed and Differential Harmonic Oscillations in Nonlinear Vibratory Systems", Memoirs of the Faculty of Engineering, Nagoya University, Vol. **18**, No. 2 (1966-11), pp. 139-149.

16) T. Yamamoto, "On the Critical Speeds of a Rotating Shaft", Jour. Japan Soc. Mech. Engrs.", Vol. **66**, No. 531 (1963-4), pp. 528-535.
T. Yamamoto, "On the Critical Speeds of a Shaft", Memoirs of the Faculty of Engineering, Nagoya University, Vol. **6**, No. 2 (1954-11), pp. 109-119.

17) Y. Shimoyama and T. Yamamoto, "On the Critical Speeds of a Shaft due to the Deflections of Bearing Pedestals", Trans. Japan Soc. Mech. Engrs., Vol. **20**, No. 91 (1954-3), pp. 215-222.
T. Yamamoto, "On the Critical Speeds of a Shaft", Memoirs of the Faculty of Engineering, Nagoya University, Vol. **6**, No. 2 (1954-11), pp . 119-133.

18) T. Yamamoto, ""Summed and Differential Harmonic" Oscillation in Non-Linear Vibratory Systems (Systems with Unsymmetrical Nonlinearity)", Bulletin of the JSME, Vol. **4**, No. 16 (1961-11), pp. 658-664.